universität wien

MASTERARBEIT / MASTER'S THESIS

Titel der Masterarbeit / Title of the Master's Thesis

„Manufacture and characterization of model micro- and nanoplastics“

verfasst von / submitted by

Markus Falkenstätter, BSc

angestrebter akademischer Grad / in partial fulfilment of the requirements for the degree of

Magister pharmaciae (Mag.pharm.)

Wien, 2023 / Vienna 2023

Studienkennzahl lt. Studienblatt / degree programme code as it appears on the student record sheet:	UA 066 605
Studienrichtung lt. Studienblatt / degree programme as it appears on the student record sheet:	Masterstudium Pharmazie
Betreut von / Supervisor:	Univ.-Prof. Dr. Lea Ann Dailey
Mitbetreut von / Co-Supervisor:	

This master thesis project was performed from March to August of 2022 at the Division of Pharmaceutical Technology & Biopharmaceutics at the University of Vienna under the supervision of Univ. Prof. Dr. Lea Ann Dailey. This thesis was realized within the “Imptox” project which received funding from the EU’s Horizon 2020 program (grant agreement n. 965173).

Abstract

For some time now, global plastic pollution has been a recognized problem. More recently, the focus has shifted to micro- and nanoplastic (MNP) pollution. These small particles are either intentionally produced or, more often, the result of a degradation process that occurs when larger plastic debris breaks down in the environment. These particles can now be found in every corner of the world and are potentially a major threat to human health. However, the knowledge of human health effects is still very limited, in part due to a lack of standardized testing materials, especially for the plastics most commonly found in humans, such as polypropylene (PP).

Within the scope of this master thesis, two approaches were investigated to produce PP particles in three different size ranges. The main part of the work was dedicated to the optimization and investigation of the reproducibility of a wet grinding process to produce particles in the size range of 1-10 µm (M-fraction) and 10-38 µm (L-fraction). This process consisted of a milling step followed by three different size separation steps including sieving, filtration, and centrifugation. The last step of the process consisted of the exchange of the suspension medium to enable the use of the suspension for cell culture experiments. Reproducibility was tested by performing the whole production procedure 5 times. In addition, a method called “non-solvent induced phase separation (NIPS) was employed to investigate the possibility to produce PP nanoparticles in the size range of 0.1 – 1 µm. The particle size distributions and percentiles were measured *via* laser diffraction and the yield was determined gravimetrically and *via* particle counting using an optical microscope.

Through optimization of the milling process, it was possible to produce particles in the desired size ranges for the L- as well as the M-fraction. The study revealed a high degree of reproducibility throughout the whole process of the L-fraction production in terms of particle size (Mean percentiles of the final L-fraction: D90: 58.78 µm ± 6.33%; D50: 27.76 µm ± 4.91%; D10: 9.35 µm ± 4.22%). In contrast, the M-fraction process was not found to be adequately reproducible (Mean percentiles of the final M-fraction: D90: 45.36 µm ± 19.12%; D50: 12.29 µm ± 10.74%; D10: 4.01 µm ± 9.81%). Concerning the final yield, the study showed a low reproducibility for both fractions (L-fraction: 3.32 ± 0.90 mg (26.99% RSD); M-fraction: 0.91 ± 0.31 mg (33.59% RSD). Furthermore, it could be demonstrated that producing PP-NPs with the NIPS method was possible (Mean percentiles: D90: 43.42 µm ± 52.66%; D50: 2.62 µm ± 63.45%;

D10: 0.312 µm ± 15.49%). The yield data of the NIPS method showed more consistency, and the relative yield was greatly increased - compared to milling - with a mean yield of 89.85% ± 2.42% (245.74mg). This study provides evidence that PP-MNP can be produced in the desired size ranges but reproducibility of size and yields vary between methods.

Table of contents

List of abbreviations

EtOH	Ethanol
HDPE	High-density polyethylene
LDPE	Low-density polyethylene
MNP	Micro-and Nanoplastics
MP	Microplastics
NP	Nanoplastics
PET	Polyethylene terephthalate
PP	Polypropylene
PS	Polystyrene
PSD	Particle size distribution
PUR	Polyurethane
PVC	Polyvinylchloride
RSD	Relative standard deviation

1. Introduction

1.1. Plastics and the Global Pollution Problem

Plastics are a group of synthetic materials with many favorable properties and a wide range of applications. However, mismanagement of plastic waste and the resulting pollution have become a global challenge. It is estimated that since the beginning of mass production until now, roughly 7,800 million tons of plastic waste have been produced. The global production keeps rising with a compound annual growth rate of 8.4% [1] and reached a new high in 2019 with almost 370 million tons in that year alone [2]. The projected production of plastics is estimated to be around 1,600 million tons per year by 2050 [3], which would raise the total waste produced to 33,000 million tons, of which only roughly half would be recycled or incinerated [1]. Such alarming forecasts call for sustainable solutions to reduce the impact on the environment.

Plastic refers to a wide range of synthetically or semi-synthetically produced polymers. These include thermoplastics, thermosetting plastics, and biodegradable plastics. Within these classifications there are several hundreds of polymers commercially available. However, there are certain polymer types, often called commodity plastics, which take up the largest share of the global demand [4]. The main types of polymers used are polypropylene (PP), high- and low-density polyethylene (HDPE; LDPE), polyvinyl chloride (PVC), polyethylene terephthalate (PET), and polyurethane (PUR) [5], [6]. These polymers have different chemical structures, which give them their unique properties. For example, polypropylene has a linear structure and is known for its strength and its high resistance to heat and chemicals, making it ideal for food packaging and applications in the automotive sector [7]. The largest end-use markets for these plastics are the packaging industry, which accounts for approximately 40% of total plastic demand, and the construction sector, which makes up roughly 20% of total plastic use. Additionally, the automotive industry and electronics and consumer industries together make up an additional 20% of end use [2].

One of the remarkable advantages of these materials is their low price and the possibility to mold them into any desired shape, making the material extremely versatile [6]. By incorporating certain additives, such as plasticizers, stabilizers, flame retardants, dyes, and lubricants into the polymers, the characteristics of the plastics can be further modified. This contributes greatly to the usefulness of these materials [8], [9]. Due to their hydrophobic nature, high molecular weight, and the absence of

chemical groups that would make them prone to enzymatic degradation, plastics ,especially polyolefins, are very durable [6]. This makes the plastics incredibly resistant to degradation processes such as corrosion and weathering [9]. Although a high durability is generally a desirable characteristic for most materials, it is also the main reason for the pollution problem. Plastics can persist in the environment for long periods of time, leading to the accumulation of plastic waste in landfills and the pollution of oceans and waterways. [9] It is estimated that there are already over 5 trillion pieces of plastic of all sizes floating in the world's oceans, with millions of tons entering the oceans every year [10]. This has led to plastic debris being discovered in every corner of the world, from all shorelines across the globe [11], to the deep sea [12], to cities [13] and even to remote areas such as mountain ranges [14] and antarctica [15]. Therefore, humans are permanently exposed to plastics. This is supported by evidence that plastics were found in the human lungs [16], [17], human stool samples [18] and the bloodstream [19]. These findings inevitably raise questions about the impact of the plastics on human health.

1.2. Micro- and Nanoplastics

In the past, the focus of scientific interest has been on macroplastics. More recently this changed and micro- and nanoscale particles have become the focal point of research.

First reports of very small plastic particles in the ocean were made in 2004 by a research group associated to marine biologist Richard Thompson [20]. To date, no standardized size classification for plastic particles exists. The size definition of microplastics varies widely between studies, as shown in Figure 1, with some researchers classifying them as particles up to 10 mm in diameter [21], while others define them as particles < 1 mm [22], [23]. However, many studies as well as the US National Oceanic and Atmospheric Administration (NOAA) refer to microplastics (MPs) as particles below 5 mm [13], [24], [25]. Particles larger than these sizes have generally been referred to as macroplastic. The term “mesoplastic” has also been introduced for particles just over 5 mm in size to further distinguish them from macroplastic particles [26]–[28]. In contrast to the wide variety of size classifications for microplastics, there are only two common size classifications for nanoplastics (NPs). Some studies define nanoparticles as particles between 1 and 100 nm [28], but there are also many defining NPs as all particles below 1000 nm [26]. The European Union Observatory for

Nanomaterials (EUON) as well as the International Organization for Standardization (ISO) use this definition [29], [30] and it is therefore used in this thesis.

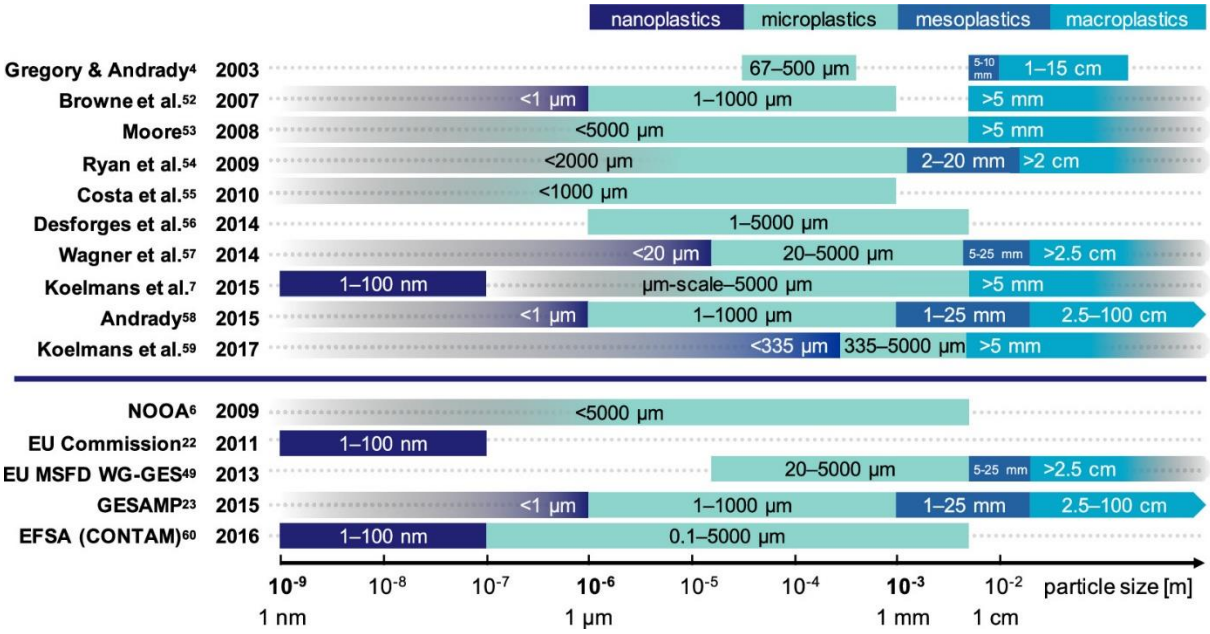

Figure 1: Different size-classifications for plastic debris found in literature. Reused with permission from Hartmann et al. [26]. *Copyright 2019 American Chemical Society.*

In general, microplastics can be categorized as primary or secondary plastic particles [28], [31], [32]. Primary microplastics are intentionally produced plastic particles. They are added to various products such as cosmetics, skin exfoliants, and toothpastes [32]. In this context, these particles are often referred to as “microbeads” that are usually made from polyethylene or polypropylene [33]–[35]. Primary microplastic particles can also be used as air blasting medium, where the particles are often additionally contaminated with heavy metals [35]. Plastic pellets that are used as raw materials for further manufacturing (typically 2-5 mm) can also be considered primary microplastics [32], although some do not include them in this category [36].

Secondary microplastics are tiny fragments of plastic that are the result of the breakdown of larger plastic debris in the environment [20], [32], [36]. Although plastics are generally considered to be very resistant, prolonged UV-exposure and mechanical stress can lead to the formation of smaller microparticles [32], [36]. UV-induced photo-oxidation of polymers plays a major role in the breakdown process [37], since it can lead to the formation of free radicals within the polymer matrix. These radicals eventually cause random chain scissions in the material, reducing the average molecular weight of the polymer chains. In addition, secondary processes such as cross-linking can occur [38]. These degradation mechanisms lead to weakening,

discoloration, and embrittlement of the material. It is thought that this process is more likely to occur on land, where sun exposure is high, and oxygen is readily available [32], [36]. When the plastics are then subjected to physical stress such as waves or wind, the actual fragmentation occurs [37], [39]. Over time, this weathering is thought to lead to the formation of smaller and smaller particles, eventually reaching the nanoscale [40]. Biodegradation by fungi, bacteria and even crustaceans may also play a role, to a lesser extent, in the fragmentation and degradation of plastics [41], [42]. In addition to the origin, primary and secondary MPs also differ in shape. Unlike primary microplastics, which are generally spherical in shape and have a smooth surface, secondary particles can vary greatly in shape and surface morphology [43].

1.3. Sources, Transport and Fate of Microplastics in the Environment

Microplastics in the environment are to a great extent the result of waste mismanagement. It is estimated that about 75-90% of the plastic waste in the oceans comes from terrestrial sources and only a relatively small percentage from ocean-based sources [44]. A major contributing factor is the particularly high population density near coastlines around the world. About half of the world's population lives within 80 kilometers of the ocean [32]. Primary microplastics enter the ocean mainly through sewage systems, while secondary microplastics enter the ocean mainly through freshwater rivers [44].

Plastic waste has reached every corner of the world. After entering the ocean, wind and ocean currents transport it to even the most remote places. It accumulates not only along shorelines and in surface waters but can be found throughout the water column including the sea floor [11], [32]. The vertical distribution in the water is related to the properties of the polymer, mainly the density of the material [45]. While lower density plastics such as PP will float on the water surface, higher density plastics like PVC will be prone to sink to the ocean floor [32], [45]. Organisms such as algae and bacteria also play a major role by adhering to the MNPs, increasing the weight of the particles, and thus favoring sinking of otherwise buoyant particles [39]. MNPs on the seabed can be re-suspended in the water column by turbulence such as storms [32].

MNPs can also become airborne in several ways. Wave action and the resulting sea spray can carry particularly small particles into the atmosphere. It is thought however, that land-based microparticles are a much larger contributor to plastic pollution in the air [44], with a large part being attributed to wear and tear from textiles like clothes or

carpets, car tire abrasion and general plastic dust from densely populated areas [46], [47]. Minor sources of airborne plastics are thought to be industrial emissions, landfills, waste incineration and the use of sewage sludge as fertilizer in agriculture [48]. Once in the air, the particles can travel very long distances, even reaching uninhabited and remote regions like the Tibetan plateau, the Pyrenees, and the poles [14], [15], [49], [50].

1.4. Exposure Pathways

Due to the ubiquitous presence of MNPs in the environment, their impact on the environment and especially on human health is of great scientific interest. There are several ways in which MNPs can enter the human body.

Probably the most notable route is oral ingestion through food or drinking water, where MNPs have already been detected [51]–[54]. Particles have been shown to partially pass through the filtration systems of wastewater treatment plants. These particles can then be released into the environment when the treated water is discharged [55]. In addition, MP-containing sewage sludge, which is often used as fertilizer in agriculture, can contaminate soils and eventually reach the groundwater, a very important source of freshwater for large parts of the world [56]. Another major source of MNP ingestion is food coming from marine sources. MNPs have been detected in organisms throughout the food chain, ranging from zooplankton at the base, to mussels, crustaceans, and fish [57]. Some studies seem to indicate that the exposure through plastic food packaging might possibly be even higher than through food coming from marine sources [58].

Another major route of MNP uptake is through air inhalation. Several studies suggest that MNPs are widely spread in the atmospheric compartment [47], [59]. *Dris et* al. (2016) showed the presence of MNPs in the atmospheric fallout of the city of Paris and surrounding areas and that these consist to a large part of synthetic fibers from textiles [46]. There is not much information available regarding the concentrations of MNPs in the air. It is assumed that the values are highly dependent on climate and seasons and are also influenced by the measurement methods [48]. Compared to the atmosphere, the concentration of airborne plastic fibers is much higher in indoor environments with synthetic materials accounting for approximately 33% of the total fiber content in the air, the rest being natural fibers such as cotton and household dust. This can be attributed to the extensive use of plastics in construction, furniture, and textiles. These

fibers are often too large to be inhaled, but the presence of nanofibers can be expected, making inhalation likely [59].

The final exposure pathway into the human body is penetration through the skin. For example, through contact with contaminated water or cosmetics. However, due to the size of most particles and their hydrophobic properties, skin penetration is very unlikely [60]. There is a possibility, though, that particles less than 100 nm in diameter may penetrate the skin [8]. Possible routes also include hair follicles, sweat glands and damaged skin areas [60].

1.5. Impact of MNP-Exposure on Human Health

Although much effort has been made in recent years to study the effects on the environment, the knowledge about the effects of MNPs on mammalian cells and especially on human health is still limited. This is particularly true for the effects that nanoplastics might have in the body [57], [60].

Since oral ingestion is the main route by which MNPs enter the human body, the translocation through the gut is of particular importance [57], [61]. It is estimated that one person on average ingests between 39.000 and 52.000 microplastic particles per year [62]. Studies have demonstrated that biologically inert microparticles ranging in size from 0.1 to 150 µm, can be taken up from the human intestine into the lymphatic system [63]. Absorption of polymeric microparticles, although limited, has also been demonstrated in *in vitro* studies using human colonic mucosal tissue [57]. The main mechanism that enables uptake from the intestine is endocytosis by M-cells. However, researchers believe that less than 0.3% of the particles ingested in this way enter the bloodstream. The remainder and particles > 150 µm are excreted in the feces [8]. The extent of uptake is strongly dependent on factors such as hydrophobicity, shape, charge, composition of the protein corona and, of course, particle size [61]. These factors also influence the ability of MNPs to accumulate in the body and their respective toxicity. Some information on the behavior of PE and PET MPs in the body is already available from research on prosthetics abrasion. These studies suggest that particles smaller than 50 µm can translocate from the lymphatic system to organs such as the liver or spleen, where they can cause inflammatory reactions. Accumulation can also happen in cells such as macrophages, therefore altering the immune system [64].

Another point of interest is the effect of airborne plastic particles on the lungs. MNPs can exert direct adverse effects on lung tissue and overall respiratory health. This is

because particles with a size of less than 2.5 µm reach the deep lung and thus can be retained. The main mechanism of toxicity is the generation of reactive oxygen species (ROS) and subsequent inflammatory processes [61]. In addition, the lung has a large alveolar surface area and a thin blood-air barrier, which can allow small particles to enter the circulation [8]. This may also depend on whether the particles are hydrophilic enough to immerse in the lung fluid. Otherwise, they will be transported out of the lung by mucociliary transport. Additional biological responses to exposure to MNPs may include genotoxicity, apoptosis, and necrosis, ultimately leading to permanent tissue damage or the development of cancer [64].

There is little information about the specific effects of nanosized plastics on human health. However, they are of special interest because they can enter cells by crossing biological membranes [57]. Nanoparticles have also been found to translocate more easily in the body and exert inflammatory reactions to a greater extent [61].

MNPs can also indirectly affect human health in various ways. One way is through the leaching of additives that are added to plastics to modify their properties. Because these additives are usually not covalently bound to the polymers, they can leach out as the plastic degrades and are then released into the environment and eventually reach humans through the food chain [8]. Substances like phthalates and bisphenol A, which are commonly used as plasticizers, are so-called endocrine disruptors in the human body, and are known to greatly impair human reproductive health [65], [66].

Another class of additives that are of concern are heavy metals. They are often added as flame retardants or coloring agents. Heavy metals can have a wide range of dose dependent negative effects on the human body. For example, many metals (e.g., Al, Sb, Pb, Cr, Hg) have a high affinity to estrogen-receptors and are therefore associated with breast cancer. Other elements like Cd, As or Hg can have cytotoxic effects or promote apoptosis or cancer [8]. Heavy metals pose not only a problem because they leach out during plastics degradation but also because they tend to adsorb to the surface of plastic particles. Multiple studies have reported elevated heavy metal concentrations together with MNPs sampled from various marine environments [67]–[69]. Heavy metal adsorption is thought to occur through the interaction of divalent metal cations or metal-oxyanions with charged or polar regions on the particle surface. The adsorption rate is increased on aged microplastics due to their surface

imperfections and particularly on small particles due to their high relative surface area [8], [64].

In addition to heavy metals, adsorption of persistent organic chemicals like pesticides, allergens and bacteria pose potential threats for human health [70], [71]. MNPs colonized by bacteria thereby could play a role in spreading microbial diseases or promote antibiotic resistance [71]. A possible connection between the exposure to MNPs and the increased occurrence of allergies is also being discussed [51].

1.6. State of knowledge

At present, it is not clear how serious the impact of microplastic pollution on the environment and human health is. In addition, pollution and human exposure are expected to increase in the future. It is therefore extremely important to understand the implications of this problem and to boost research in this area. Multidisciplinary approaches are needed to develop adequate methods to detect, identify and characterize MNPs and their potential adverse effects they might have [72].

Several studies have shown that PP is one of the polymers that are the most abundant in human stool samples as well as in human lungs and human blood. [16], [18], [19]. Therefore, this material has been chosen as representative material for the IMPTOX project within which this thesis was written. The overall aim of this project is the investigation of the ability of MNPs to modulate the response to food and respiratory allergens and the ability to bind harmful pathogens and toxins [72]. For this purpose, model-MNPs with well-defined physiochemical properties, in three size ranges (0.1–1 µm, 1–10 µm, 10–38 µm) are needed.

To determine the exact effects of inhaled or ingested MNPs in adequate *in vitro* and *in vivo* assays, standardized and well-characterized plastic particles are needed. Isolating those particles from the environment is often not a viable option, as it is not always possible to collect MNPs in sufficient quantities and with sufficient size separation. This is especially true for small MPs and NPs. In addition, pristine particles that are either free of contaminants or have a known level of contamination (e.g., endotoxin concentrations) are needed to compare the effects of these MNPs to their native counterparts [72].

As highlighted by Eitzen *et al*. [73], there are commercially available plastic particles of the polymers of interest. However, many of them come in sizes from 1 – 5 mm which

could be technically considered as microplastic. In general, though, smaller particles are considered more relevant for toxicological investigations since their impact on human health and the environment is expected to be much greater. There are also some commercially available micro- and nanoparticles in the wanted size ranges, but these often come in form of suspensions which are stabilized by surfactants and in addition have a spherical geometry and therefore do not resemble the MNPs found in the environment [73]. Additionally, their high cost and reliance on supply chains are crucial limiting factors [72].

Furthermore, many studies in the past only investigated the effects of polystyrene (PS) particles, mainly because PS is easy to handle and produce and because PS particles can be efficiently dispersed in water [74], [75]. Thus, there is a demand for well-defined PP and PET test materials in the micro- and nanometer size range, which can be used to validate and calibrate analytical methods, which is especially important for the analysis of nanoplastics in the environment [76], [77], and to assess the effects of these particles on human health.

1.7. Possible Approaches of MNP Production

Due to their special characteristics, it is particularly challenging to produce model MNPs that match particles found in the environment. Sampled MNPs are often found to be very irregular in shape, oxidized on their surface and often are covered in biofilms [78]. There are mainly two ways to produce MNPs. Either by bottom-up generation or from top-down. Several techniques are available for both approaches, such as polymerization and precipitation for bottom-up production, and mechanical grinding, ultrasonic treatment, and melting for top-down MNP production. The process behind the MNPs occurring in the environment belongs to the latter category [43]. The top-down approach is therefore particularly advantageous. In the case of mechanical grinding, it is possible to produce particles in most size-ranges in a cost-effective and easily accessible manner.

There is also a third method of MNP production that cannot be adequately attributed to neither the top-down nor the bottom-up approach known as non-solvent induced phase separation (NIPS). The difference is that with NIPS, the particles are formed through a physical process by adding a non-solvent to decrease the solubility, while in bottom-up methods such as polymerization, the monomers chemically react to form the polymer chains. [79].

1.7.1. Mechanical Grinding

Mechanical grinding or milling is a widely used top-down process for size reduction of solid materials. In this process, large particles are crushed by four acting forces. These are shear, impact, compression, and friction [80]. All comminution processes are characterized by the fact that new surfaces are created, which are several magnitudes greater than the original surface area. The energy required to grind solid materials is dependent on their composition as well as the type of chemical bond that needs to be broken. In addition, the required energy is influenced by the new surface area and mainly determined by the target size of the particles. Generally, the creation of smaller particles requires more energy input. The arrangement of molecules or atoms of the material is an indicator for how the material is deformed under mechanical stress. This behavior can be well described by a stress-strain-curve, which shows the deformation path (strain) of a material in relation to the force per unit area that is required to break it (stress) [81], [82]. Brittle materials, such as salts or minerals, can only be deformed to a very small extent, because of their ionic bonds. The application of mechanical stress causes a shift in the orientation of the ions, causing ions of the same charge to face and thus repel each other, which leads to the breaking of the material. Plastics exhibit what is known as elastic-plastic behavior. This means they initially react elastically under stress but return to their original shape once the stress is relieved. However, if the stress is increased to a certain point the material begins to deform permanently. This is due to the polymer chains shifting against each other, relieving some of the stress in the process [82].

Plastic deformation can be influenced by high stress velocity. If the material is deformed rapidly, there may not be enough time for the internal structure to rearrange to relieve the stress, causing the material to become brittle for a short period of time [82]. Another way to influence the behavior of a material during grinding is through cooling. Operating below the glass transition temperature is particularly important here [43], [83], [84]. Low temperatures reduce the ability of the polymer chains to rearrange and result in embrittlement. The energy required for cooling is hereby often less than the energy required for comminution at normal temperatures [82]. Cooling can also minimize the risk of melting or degradation of the material during the milling process [85].

Due to the high energy that is required for the comminution of plastics, cutting mills or mills that exert impact forces are generally best suited [86]. Milling in combination with some forms of cooling have been used in various studies to produce MPs and NPs. However, the particle sizes achieved were mostly > 200 µm [73], [87]–[90]. More recent efforts to achieve smaller particles were applying cryogenic wet grinding [86], [91], [92]. It is believed that by using a wet milling process, the particles resemble those found in the environment more closely [92]. It can therefore be assumed, that a wet milling method in combination with embrittlement by cooling is the most suitable for producing model MNPs with the desired characteristics.

1.7.2. Nonsolvent-induced phase separation (NIPS)

Bottom-up production is a process often used in the industrial production of MNPs. These processes can be divided into chain-growth polymerization and step-growth polymerization. Polyesters for example, are produced by step-growth polymerization, while PP is generally produced *via* chain-growth polymerization [43]. However, there is also a different and easy-to-use approach, called nonsolvent-induced phase separation to produce these kinds of particles. This is a dissolution and reprecipitation technique, comprised of three components (polymer, solvent, nonsolvent), that is often used to create polymer membranes [93]. However, this technique can also be used to produce NPs, as Lee *et al.* have shown. They used xylene to dissolve the PP and ethanol as a nonsolvent to recrystallize the dissolved PP. A major advantage of this technique is the high yield of NPs compared to grinding. It is also less time consuming and does not require complicated and expensive equipment [79].

1.8. Aims of the thesis

The focus of this thesis was to investigate the reproducibility of a top-down production approach to produce model polypropylene MNPs that can be used as testing material for the “IMPTOX” project in the EU Horizon 2020 program. The overarching aim was to produce model MPs between 10 -38 µm and 1 – 10 µm, which were subsequently labelled as the L- and M-fraction respectively, and NPs with a size < 1 µm. To achieve this, the preexisting production process was optimized and then carried out 5 times to evaluate the reproducibility of the resulting L-fraction and M-fraction and the ability to produce submicron particles. In addition, the NIPS-technique to produce nanoparticles was employed and its feasibility was investigated.

2. Materials and Methods

2.1. Chemicals and Materials

Ethanol 96% was purchased from Brenntag Austria GmbH (Vienna, Austria). Anhydrous glycerol for synthesis (8.18709), Tween® 80 (P1754) and isotactic polypropylene (427888) with an average Mw of ~250.000, an average Mn of ~67.000 and a density of 0.9 g/mL at 25 °C were purchased from Sigma- Aldrich (Saint Louis, Missouri, USA) and xylene for analysis was purchased from Merck KGaA (Darmstadt, Germany).

2.2. Production methods

Two methods were employed to prepare the PP-MNPs in three size classes. The first method involved using a knife mill followed by size separation *via* filtration and centrifugation, targeting the size ranges L (10-38 µm) and M (1-10 µm). The second method (NIPS) was used to produce the S-fraction (<1 µm).

2.2.1. Particle production via milling

The production of PP particles by milling involved a 5-step process shown in Figure 2. This includes pre-treatment of the native PP pellets, mechanical comminution, subsequent size separation and lastly a medium exchange from EtOH to glycerol. The details of each step are outlined in the following sections.

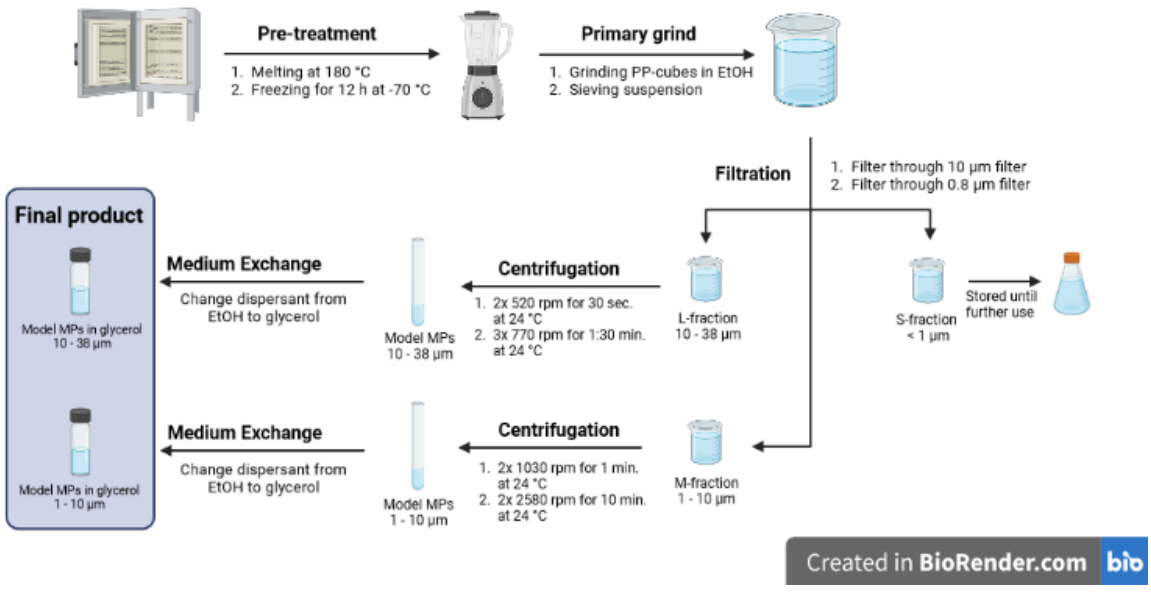

Figure 2: Schematic representation of the final production process for L- and M-fraction model PP-particles. Created in BioRender.com

2.2.1.1. Pre-Treatment

To ensure uniformity of the starting material, the polypropylene pellets were melted into cuboids (1x1x0.2 cm). A silicone mold with 160 chambers was used and 8 pellets were added per chamber. The PP was then heated in an oven at 180°C for 1 hour. After cooling down to room temperature, the PP cuboids were stored in a freezer (Deep Freezer 6481, GFL Technology, Burgwedel, Germany) at -70°C for at least 12h. This embrittled the material for increased grinding efficiency.

2.2.1.2. Primary Grind and Sieving

The frozen PP cuboids were transferred into the milling chamber of a knife mill (GM 200, Retsch GmbH, Haan, Germany) and EtOH (96%, 40 mL) was added. Subsequently, milling was carried out using the hit mode (1 min, 4.000 rpm), where the knives rotated backwards and crush the material with the blunt side. After a 2 minutes break to cool down, the mode was changed to cut (knives rotating forwards at 10.000 rpm). EtOH (96%, 5 mL) was used for rinsing and the material was milled one more time. Thereafter, a volume reduction lid was employed to enhance contact time with the knives. The material was milled 5 more times under the same conditions. After each cycle, an additional 5 mL of EtOH was added to the milling container for rinsing.

For a first separation step, the PP-EtOH mixture was transferred to a sieve tower. The setup consisted of a base stainless-steel pan, a vibratory sieve shaker (Rhewum, Remscheid, Germany) and 5 sieves in total. From top to bottom, the mesh sizes used were: 800 µm, 500 µm, 180 µm, 63 µm and 38 µm (Retsch GmbH, Haan, Germany). To break aggregates, sieving aids were added on top of each sieve (ZrO_2, steel). The material was then sieved (5 min, Intensity 7, Interval 7) and the resulting fraction in the collecting pan (LMS-fraction, <38 µm) was transferred into a pre-weighed clean glass beaker. A sample of 400 µl of the LMS-suspension was taken and transferred into a small vial for particle size distribution analysis.

2.2.1.3. Filtration

To further divide the LMS-fraction, the material was filtered two times *via* vacuum filtration. In the first step, the LMS-fraction was filtered through a 10 µm nylon mesh filter (Merck-Millipore, Burlington, Massachusetts, USA). The filter was then transferred into a clean beaker and 20 mL of EtOH (96%) were added. The beaker was then sonicated in an ultrasonic water bath (Elmasonic P 30 H, Elma Schmidbauer GmbH, Singen, Germany) for 5 minutes to detach the particles from the filter. After sonication,

the filter was discarded, and the resulting L-fraction (10-38 µm) was stored in a beaker until further use. The filtrate from the first filtration step was filtered again through a 0.8 µm nylon membrane filter (Whatman plc, Maidstone, UK). The filter was transferred into a clean beaker and 10 mL of EtOH (96%) were added. The beaker was sonicated for 5 minutes to resuspend the particles and the filter was discarded thereafter. A sample of 400 µl of the L- and M-suspension respectively were transferred to a small vial for later characterization.

2.2.1.4. Measurement of particle size distribution

The measurements of the particle size distributions were conducted *via* static light scattering (Mastersizer 3000, Malvern Panalytical, Malvern, United Kingdom). Sample preparation was necessary for reproducible measurements. To prevent aggregation of PP particles in the aqueous environment of the measurement chamber, a Tween® 80 solution (5%, w/w, in DI-water) was added to the sample in a 1+1 ratio. Particle-free water (6 mL) was added to the measurement cell followed by 400 µl of Tween® 80 solution (5%, w/w, in DI-water). The sample was kept in the sonicator during measurement preparations and vortexed shortly before adding the sample to the measurement cell. The sample was added in increments of 50 µL until a laser obscuration of 5-10% was reached.

As a scattering model to calculate size-distributions, the Mie-theory was used. The measurement parameters were as follows: the stirring speed was set at 700 rpm, for the dispersant the refractive index of 1.33 for water was chosen. The particle shape was set to non-spherical for the milled material and spherical for precipitated particles. A refractive index of 1.49 and an absorption index of 0.01 were selected for the polypropylene particles. Each sample was measured 10 times and the results were reported as the average of these measurements. The results were plotted as a particle size distribution (PSD) curve with the x-axis representing the particle diameter and the y-axis representing the volume density at the respective size. In addition, the 10th, 50th and 90th percentiles were calculated and reported as D10, D50 and D90 values. Furthermore, the uniformity-value of the PSD was reported, which was an indicator for the spread of the size distribution. Narrow distributions show a low uniformity value while a high uniformity value indicates a broad PSD.

2.2.1.5. Concentration determination

To determine particle concentrations a gravimetric method was used. A sample of 1 mL suspension was taken and transferred into a pre-weighed Eppendorf tube (Safe-Lock microcentrifuge tube, 2 mL, Eppendorf, Hamburg, Germany). The weight was determined, and the weight of the suspension added was calculated. The tube holding the suspension was then connected to a rotary evaporator (Rotary Evaporator VV 2011, Heidolph Instruments GmbH & co, Schwabach, Germany) and lowered into a water bath (60°C). The pressure was slowly reduced in increments of 100 mbar over the course of 1 h until complete dryness. The tube was weighed again, and the weight of the remaining PP was determined.

The sample concentration was calculated according to equation (1).

$$conc.\left(\frac{mg}{g}\right) = \frac{Tara\ +\ PP - Tara}{(Tara + Suspension\ -\ Tara)\ *\ 1000} \quad (1)$$

2.2.1.6. Centrifugation

To reach the desired particle size distributions (PSDs), further fractionation employing centrifugation of the filtered L- and M-fractions was necessary (as shown in Figure 3 and Figure 4). After sonication (> 1 minute) the L-fraction was divided equally and transferred into 4 clean centrifugation tubes (11.5 mL, Pyrex®, Corning, Inc., New York, USA). Filtered EtOH (96%) was then added to the tubes (1+1), each tube was weighed and if necessary additional EtOH (96%) was added to reach the same weight for each tube (30g). This weight balancing step was carried out before each new centrifugation run. Centrifugation was carried out using a benchtop centrifuge (Rotanta 460 R, Hettich Instruments, Beverly, Massachusetts, USA) with a swinging bucket rotor (5699-R = 196 mm, swinging-bucket, max. speed: 4600 rpm). To exclude particles over 38 µm, the L-fraction was centrifuged at 60 rcf (520 rpm, 24°C, 30 sec). The supernatant of each tube was carefully transferred to 4 clean tubes and filtered EtOH (96%) was added until 30g was reached. The tubes were vortexed and sonicated (1 min), and the centrifugation process was repeated under the same conditions.

After excluding larger particles, the supernatant was transferred to 8 clean tubes to dilute the sample further and enhance the clean-up process of particles < 10 µm. Three more centrifugation steps at 130 rcf (770 rpm, 24°C, 1.5 min) were subsequently carried out. After the first two runs the supernatant was discarded. After the third

centrifugation run the supernatant was discarded again and the sedimented particles were collected in a glass vial. Finally, the PSD and concentration were measured.

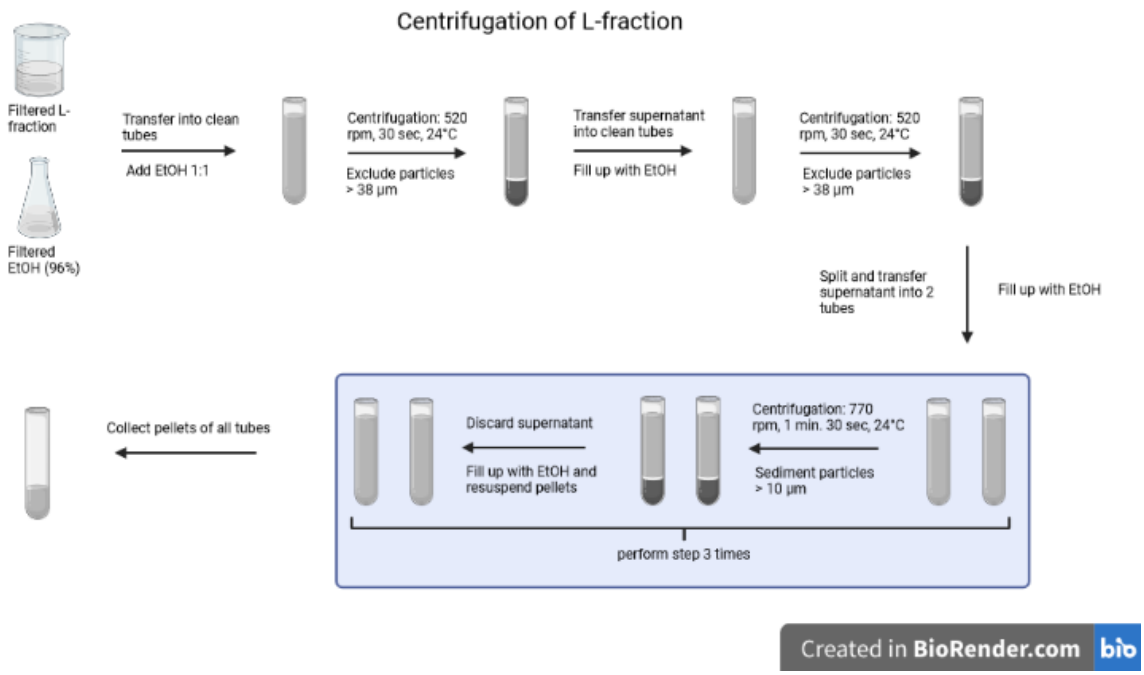

Figure 3: Schematic representation of the centrifugation process of the L-fraction. Created with BioRender.com

In a similar process, the filtered M-fraction was treated. The suspension was split and transferred equally into 2 clean centrifugation tubes. Filtered EtOH (96%) was added to reach 30 g of total weight per tube and a 1:1 ratio of sample and EtOH. The tubes were vortexed and sonicated for 1 min and centrifuged immediately. Two centrifugation steps at 232 rcf (1030 rpm, 24°C, 1 min) were carried out to exclude particles > 10 µm. After each step, the supernatant was transferred to two clean tubes and filtered EtOH was added to balance the weight. Subsequently, all particles < 1 µm were removed by carrying out two more centrifugation runs at 1459 rcf (2580 rpm, 24°C, 10 min). After the first run the supernatant was discarded and the tubes were refilled with filtered EtOH (96%). Following the second run, the supernatant was discarded again but this time the sedimented particle pellets were collected and stored in a glass vial for subsequent characterization and use.

Figure 4: Schematic representation of the centrifugation process of the M fraction. Created with BioRender.com

2.2.1.7. Yield Determination and Dispersant Exchange

The samples were vortexed and sonicated (1 min) and transferred to a pre-weighed Eppendorf tube. Using a rotary evaporator (water bath at 60°C), the EtOH was evaporated over the course of 30 to 60 minutes by gradually decreasing pressure. The processed tube was then weighed, and the total yield was determined using equation (1).

Exchanging the dispersant started with pre-heating glycerol to 70°C in a water bath. The dried PP in the microcentrifuge tube was resuspended in approx. 1 mL of filtered EtOH (96%) by alternately vortex and sonication. When the PP was dispersed evenly in the tube, the amount of glycerol needed for the desired concentration was calculated as shown in equation (2).

$$glycerol\ (g) = \frac{PP\ (mg)}{desired\ conc.\left(\frac{mg}{g}\right)} \tag{2}$$

The glycerol was transferred to a round bottom flask and the PP suspension was added while the glycerol was still hot. The flask was vortexed and sonicated until the content was distributed evenly. Employing a rotary evaporator (water bath at 70°C), the EtOH was removed by gradually decreasing the pressure (increments of approx. 100 mbar) over the course of 3 h until a pressure below 10 mbar was reached. Regularly the flask was weighed, and the process was considered complete when the weight of the flask did not change more than 1% for 2 consecutive measurements.

2.2.1.8. Microscope Imaging and Particle Counting

To get an approximation of the particle concentration, the PP suspension was sonicated for 1 minute to disperse the particles and 10 µl were transferred onto a hemocytometer. For imaging and counting, a widefield microscope (ZEISS Primostar 3, Carl Zeiss, Oberkochen, Germany) was used. Images of the particles in the 4 outer corner grids were taken and the particles were counted manually. This step was repeated on the opposite side of the counting chamber resulting in a total evaluation of 8 squares per sample. The concentration of the sample was then calculated from the mean number of particles per square as shown in equation (3). The dilution factor was assumed to be 1 as the sample was not diluted before counting and the volume per corner square was 0.0001 mL. The information was taken from hemocytometer.org [94].

$$particle\ conc.\left(\frac{particles}{ml}\right) = \frac{average\ particles\ per\ square * \ dilution\ factor}{square\ volume\ (ml)} \tag{3}$$

To gain additional information on particle characteristics like size, shape and possible aggregation, images were taken using regular microscope slides. For more information about the sample concentration, an automated particle counter (TC20 automated cell

counter, Bio-Rad Laboratories, Hercules, California, USA) was used. To measure the particle concentration per mL of sample, 10 µl were applied onto the test slide and automatically measured. This measurement could only be performed with the L-fraction because the counter was limited to particles > 5 µm.

2.2.2. Nonsolvent-Induced Phase Separation

2.2.2.1. Precipitation

The method used to acquire PP-MNPs involved the dissolution and subsequent precipitation of polypropylene. The method was adopted from Lee *et al.* [79], but temperature, cooling time and the precipitation process were slightly modified. PP pellets (approx. 0.260 g) were introduced into a round bottom flask (100 mL) and xylene (40 mL) was added. The flask was attached to a reflux cooler and placed into a silicone oil heating bath. The mixture was heated for 30 min (135°C) while stirring (250 rpm) until complete dissolution of the PP pellets. After the temperature was reached, the mixture was stirred for another 30 minutes until the PP was completely dissolved. A glass pipette (10 mL) was used to slowly precipitate the hot solution into 200 mL of filtered EtOH (96%) stirred at 400 rpm in a beaker. The beaker was covered and stirring was continued for another 15 minutes to let the suspension cool down.

2.2.2.2. Filtration and Resuspension

To remove xylene from the suspension, the sample was filtered through a 0.8 µm nylon filter (Whatman plc, Maidstone, UK) by vacuum filtration. The particles were then washed with 100 mL of filtered EtOH (96%) at least 3 times while crushing particle conglomerates manually with a spatula, to guarantee a better washing. A pre-weighed glass vial (20 mL) was filled with 13 mL of filtered EtOH (96%) and the total weight was noted. After the washing was completed, the filter was transferred into the glass vial and completely submerged in the EtOH. The vial was sonicated for at least 5 minutes to detach the PP from the filter and resuspend it. Subsequently, the filter was removed, and the vial was weighed again to determine the total yield of the suspension.

2.3. Statistical Analysis

Statistical analysis was performed with Microsoft® Excel® for Windows (Version 2304). All mean values were given with standard deviation. Statistical significance was determined using ANOVA single factor analysis and was considered statistically significant at p-values ≤ 0.05.

3. Results and Discussion

3.1. Optimization of the manufacturing process

3.1.1. Sieving

After the milling process was completed, sieving was necessary as a first step to narrow down the PSD. Because the resulting yields were very low, the sieving conditions were investigated. It was assumed that the number of sieving steps and thus the total sieving time was the parameter that had the main influence on the yield and the PSD of the LMS-fraction. It was thought that multiple sieving steps would increase the yield but also increase the likelihood of fiber-like particles – smaller than 38 µm in width but larger in length – passing through the sieve, ultimately resulting in higher mean D10, D50 and D90 values.

In total, 4 different approaches were evaluated: a single sieving step (Figure 5A), two sieving steps with resuspension in ethanol in between (Figure 5B), five sieving steps with resuspension in between (Figure 5C), and a partial sieving approach in which the sample was divided into two parts and sieved separately (Figure 5D). Each sieving step took 5 minutes to complete.

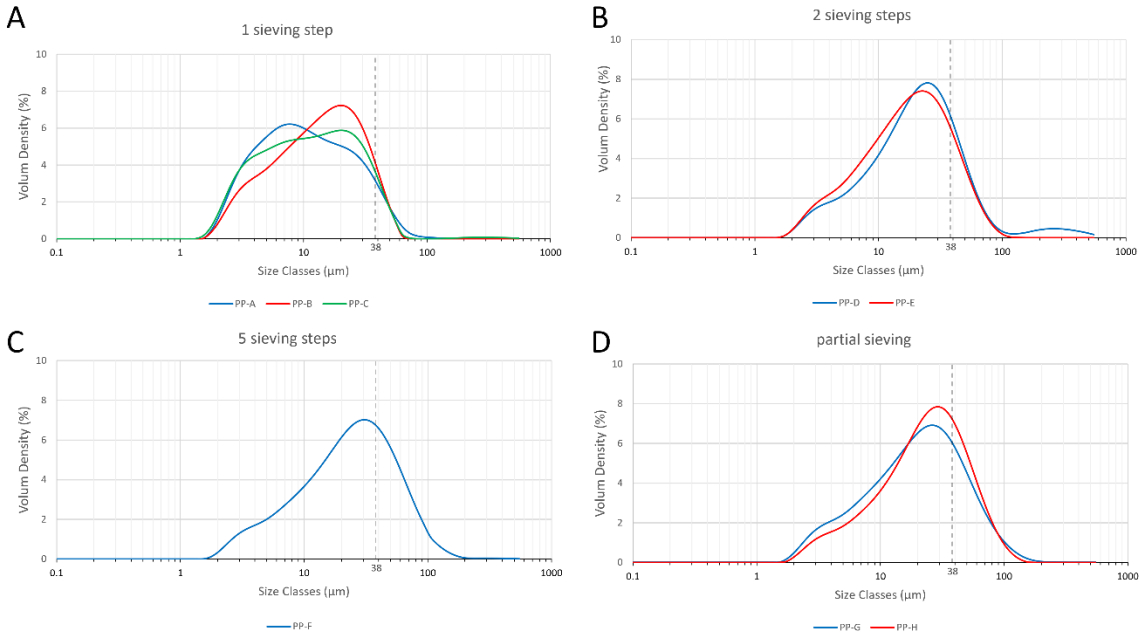

Figure 5: A) PSD of the LMS fraction of three samples sieved in one step for 5 minutes compared to B) PSD of the LMS fraction of two samples sieved in two steps for 5 minutes, C) PSD of LMS of one sample sieved in 5 steps for 5 minutes and D) PSD of the LMS fraction of two samples sieved with partial sieving.

Although the PSD for the 1-step sieving is irregular within its 3 replicates, when considering the peak of the distribution and the shape of the curve, a slight shift of the

peak towards larger particle sizes for methods that applied more than one sieving step can be observed. This suggests that more sieving steps (longer total sieving time) lead to larger particles passing through the sieve. The 1-step sieving method was associated with significantly smaller mean values in the D10, D50 and D90 percentiles compared to the other methods (*P < 0.05, *P < 0.05, P**<0.01, respectively). In addition only in the 1-step sieving method, the D90 value was in the desired size range. A comparison of these values can be observed in Figure 6.

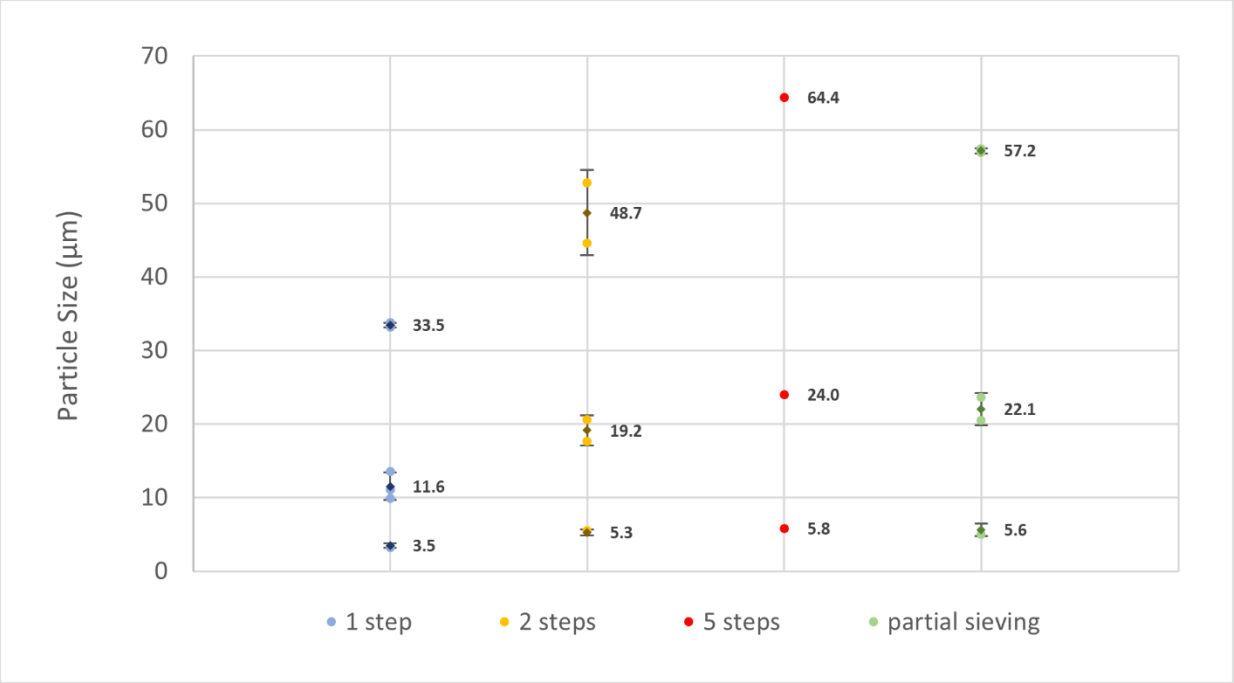

Figure 6: D10, D50 and D90 percentiles inlcuding mean values ± standard deviation of 1 step sieving (n=3), 2 step sieving (n=2), 5 step sieving (n=1) and partial sieving (n=2).

As shown in Figure 7, the mean yield (%) was higher for the sieving methods that used more than one sieving step, except for partial sieving. However, all those yield-values have a relatively large RSD (1 step = 54.5%; 2 steps = 22.3%; partial sieving = 47.8%) and the increase in yield was considered too small (1 step = 0.40% of the starting material *vs*. 5 steps = 0.72% of the starting material) to justify the increased time required to produce the particles (5 minutes of sieving *vs*. 25 minutes of sieving) and the overall poorer PSD. Therefore, it was ultimately decided to continue with the 1 step sieving method.

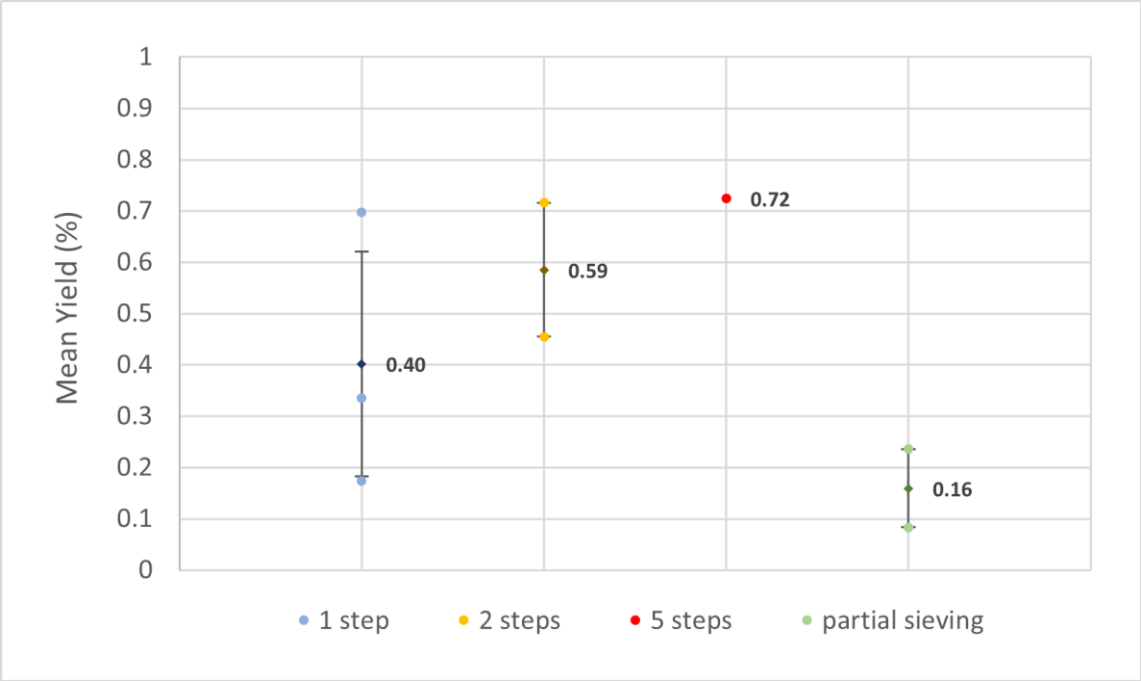

Figure 7: Relative yield including mean values ± standard deviation of the resulting LMS fraction in % of the 1 step sieving (n=3), 2 step sieving (n=2), 5 step sieving (n=1) and partial sieving methods (n=2).

In addition, it must be noted that the quality of the data is limited due to the low number of replicates and an uneven distribution of replicates across methods. To confirm these findings, a future study with a larger sample size and a more balanced distribution of replicates across methods is needed.

3.1.2. Centrifugation

Centrifugation was the final and most critical production step to fine-tune the PSD after filtration. The aim of these preliminary experiments was to optimize the process to achieve the desired size classes for the M-fraction (1-10 µm) and the L-fraction (10-38 µm) by tweaking rotational speeds and the number of centrifugation runs. The process generally consisted of one cycle in which the larger particles were removed and one cycle in which the desired particles were gathered while the smaller particles were discarded. Initially, a centrifuge with a fixed angle rotor (Rotanta 460 R, Hettich Instruments, Beverly, Massachusetts, USA) was used to approximate the necessary rcf for both centrifugation cycles. To facilitate the handling of the PP-pellets in the centrifuge tubes, the centrifuge was subsequently changed to a superspeed centrifuge (Sorvall Lynx 6000, Thermo Fisher Scientific, Waltham, Massachusetts, USA), where a swinging bucket rotor (BioFlex HC, r = 209 mm, swinging-bucket, max. speed: 5500 rpm) was available. This was done because in the fixed angle rotor, the pellets would stick to the tube walls and be easily destroyed during the manual pipetting steps.

While the process was optimized over the course of 10 samples in total, for clarity and ease of interpretation, a subset of 5 samples was selected to represent the overall optimization progress for both the L and M-fractions. The resulting PSDs can be observed in Figure 8.

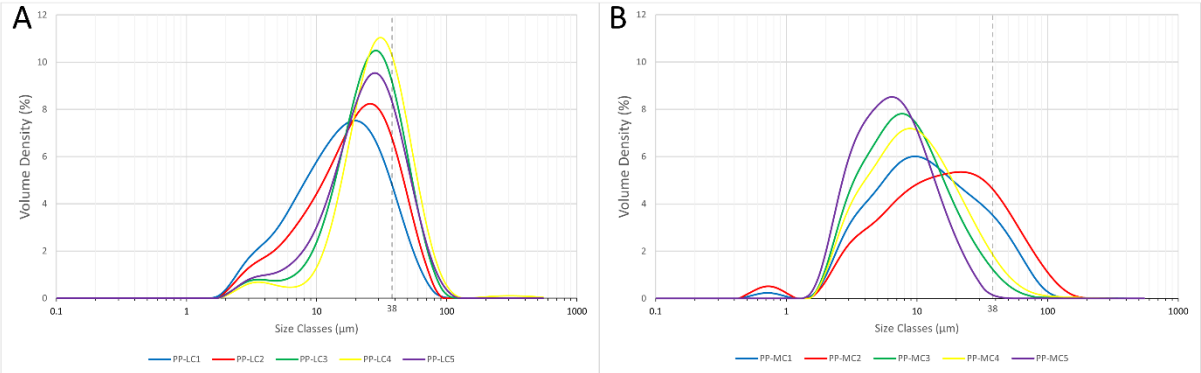

Figure 8: PSD of the centrifugation optimization process for A) the L-fraction and B) the M-fraction (n=5).

For the L-fraction, samples PP-LC1 to PP-LC3 were used to approximate the necessary rotational speeds and time with the fixed angle rotor. When looking at the PSD in Figure 8A, the progress in the centrifugation protocol can be observed. Sample PP-LC3 represents the ideal centrifugation protocol to achieve the best size distribution possible with this rotor. This becomes apparent when viewing the percentiles values shown in Table 1. At this point in the process the centrifugation protocol consisted of 2 runs to remove large particles and 4 runs to remove particles below the target range. After this, the centrifuge and rotor were changed, and the same protocol was applied. The advantage of using a swinging bucket rotor becomes apparent when viewing sample PP-LC4, which achieved an even better size distribution, especially in terms of the D10-value, which rose from 10.4 µm to 13.2 µm. However, to strike an important balance between quality of the final product and the final yield, it was decided to reduce the number of centrifugation runs from 4 to 3 in the second cycle because more runs would also decrease the yield of the final product. The final protocol, which was subsequently used for production is represented by sample PP-LC5. The optimization process proved effective in reducing the amount of particles < 10 µm, as shown in Figure 8A. The apparent increase in the D90 value, even though large particles were also removed, could be attributed to the shift in the ratio of small to large particles.

Table 1: Percentile values of 5 representative samples of the centrifugation optimization process of the L-fraction.

Sample	D10 (µm)	D50 (µm)	D90 (µm)
PP-LC1	4.83	15.8	39.0
PP-LC2	5.75	20.1	45.4
PP-LC3	10.4	26.0	51.3
PP-LC4	13.2	29.5	57.8
PP-LC5	8.53	24.8	52.0

Samples PP-MC1 and PP-MC2 were produced using the fixed angle rotor, while samples PP-MC3 to PP-MC5 were produced using the swinging bucket rotor. Changes of the M-fraction protocol can be observed in Figure 8B, where switching the rotor type is clearly visible in the PSD. Especially for the D90 percentile, the jump from values above 40 µm to values below 30 µm (Table 2) highlights the impact of the rotor change. Centrifugation parameters were further tweaked from sample PP-MC3 to PP-MC5 until a sufficient result was achieved. PP-MC5 represents the final protocol, displaying the best PSD and sufficiently precise percentile values.

Table 2: Percentile values of 5 representative samples of the centrifugation optimization of the M-fraction.

Sample	D10 (µm)	D50 (µm)	D90 (µm)
PP-MC1	3.43	11.3	41.7
PP-MC2	3.65	15.7	55.8
PP-MC3	3.15	7.92	22.5
PP-MC4	3.31	9.13	27.3
PP-MC5	2.82	6.39	15.7

Overall, this optimization process was critical to obtain samples in the desired size ranges. Especially the change from a fixed angle rotor to a swinging bucket rotor proved to be a great advantage. In addition, an important balance was struck between yield and quality of the product. However, it should be noted that in future studies, where more starting material is available and yield is thus a lesser concern, it may be interesting to revisit the protocol that was used to produce PP-LC4. The resulting centrifugation protocols developed in these experiments were used for further particle processing.

3.2. Reproducibility of milled PP

Once the production process was sufficiently optimized, reproducibility was investigated by manufacturing 5 batches of L- and M-sized PP MPs. The final production process is outlined in section 2.2.1.

3.2.1. Milling and Sieving

Milling was the first step after the pre-treatment to actually produce PP particles. This resulted in the LMS-fraction, which consisted of all particles that passed through the 38 µm sieve of the sieve tower. Subsequently, the yield was determined and the PSD was measured (Figure 9).

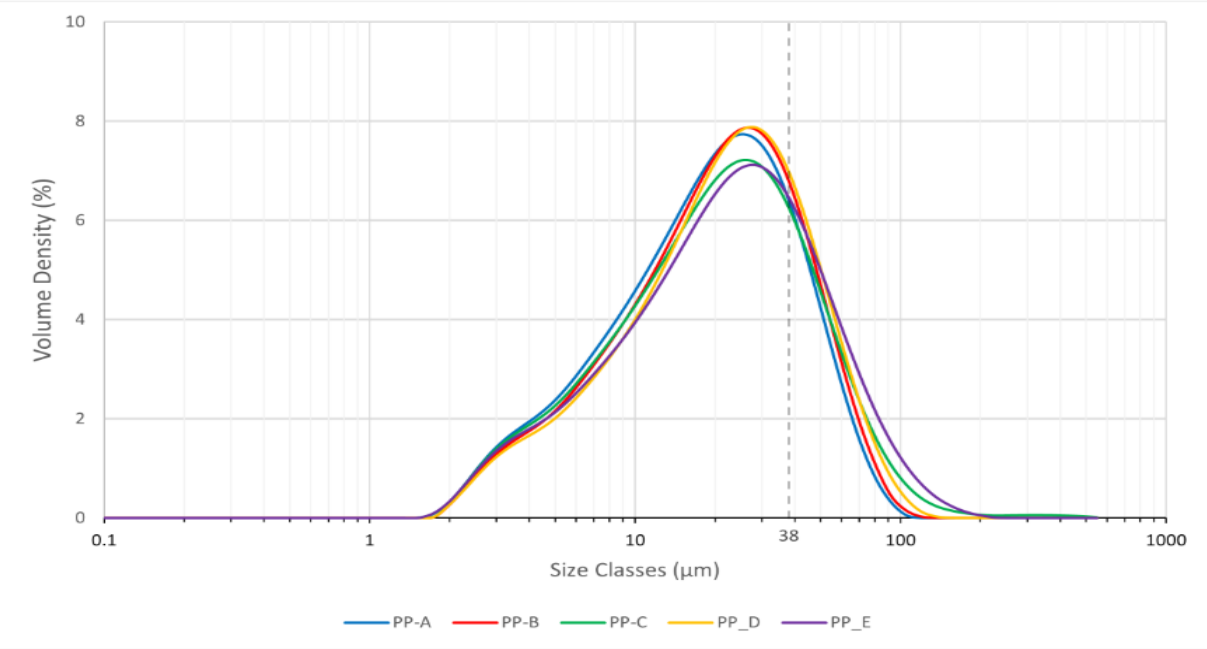

Figure 9: PSD of the LMS-fractions of samples PP-A – PP-E after the milling- and sieving-process (n=5).

The PSD of the 5 *samples* look relatively similar with the major peak at around 30 µm. However, some small differences can be seen as the volume density at the peak of the PSD of samples PP-C and PP-E is slightly lower than that of the other samples. Interestingly, these two replicates are also the ones with the comparatively highest yield (PP-E: 133 mg and PP-C: 95 mg vs PP-A: 60 mg; PP-D: 47 mg and PP-B: 29 mg), suggesting that the larger particles may be the reason for this increased yield. The PSDs of these two samples also exhibit a lower uniformity, which could imply that a greater yield can also lead to less consistent size distributions. Moreover, no submicron particles were detected in these measurements.

When comparing the D10, D50 and D90 values of the LMS fractions shown in Figure 10A, relatively low RSD values can be observed, which can be considered consistent across all replicates. Despite a slightly higher RSD in the uniformity of the samples (Figure 10B), these results indicate a high degree of reproducibility for the milling and

sieving step. However, when looking at the yield data (Figure 10C), the previously mentioned differences can be observed. The mean yield of 73.02 mg can be considered very low. Regarding the approximately 20 g of starting material, the yield is only 0.38% and has a high RSD of 50.57%. One potential reason for these differences and the high variability in the yield could be human error when operating the blender since the procedure contained many manual cleaning and rinsing steps. Another reason could be inaccurate yield measurements. The yield was calculated by first gravimetrically measuring the concentration of the LMS suspension. This was done using an analytical balance with an error of ± 1 mg. Since the LMS-suspension had a relatively low concentration, the resulting weight of the dried PP was also very low, often lying within the error of the balance. Thus, the significance of the yield data is considerably limited.

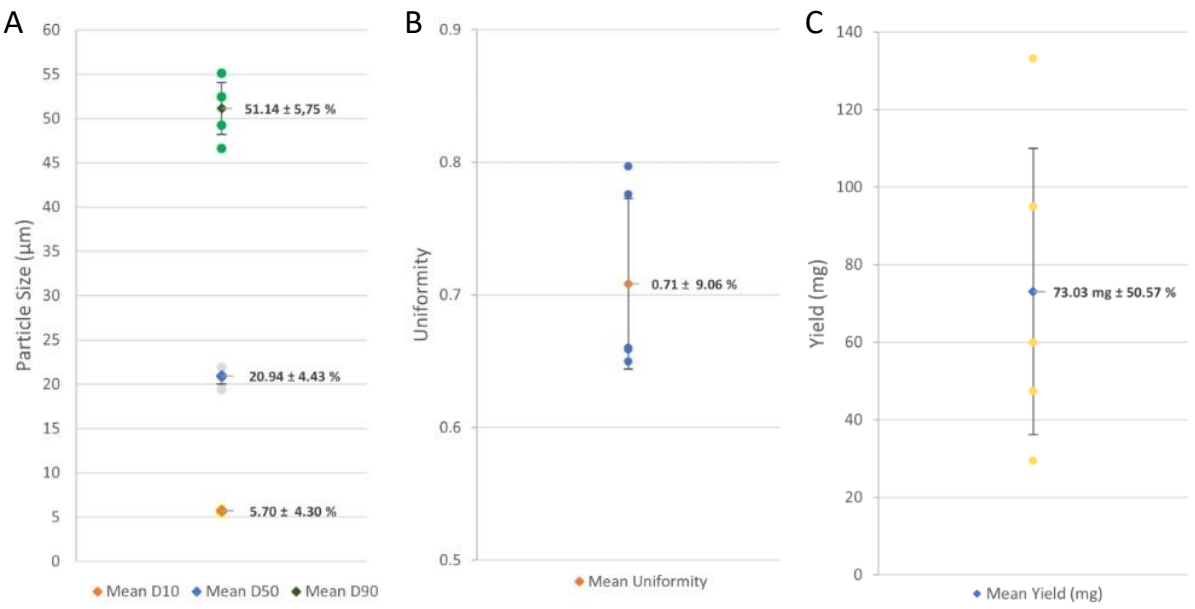

Figure 10: Reproducibility data of the LMS-fraction (n=5): A) D10, D50, and D90 percentiles including mean values ± RSD of the LMS-fraction. B) Uniformity of the PSD including the mean value ± RSD. C) Yield in mg including the mean value ± RSD.

Future studies would have to find a way to determine the yield more accurately, either by taking a larger amount of the sample and measuring it with the same technique or by using other methods. In addition, it could be studied how to increase the yield or reuse the discarded plastics. It should also be investigated if there are nanoparticles present in the LMS-fraction.

3.2.2. Reproducibility of the L-fraction

3.2.2.1. Filtration

Filtration was the second step after sieving to separate the particles by size. The LMS fraction was first filtered through a 10 µm filter. The PP that remained on top of the filter was resuspended, resulting in the L-fraction.

Looking at the measured PSD of the L-fraction shown in Figure 11, it can be noted that these 5 samples are very similar and show optimal reproducibility.

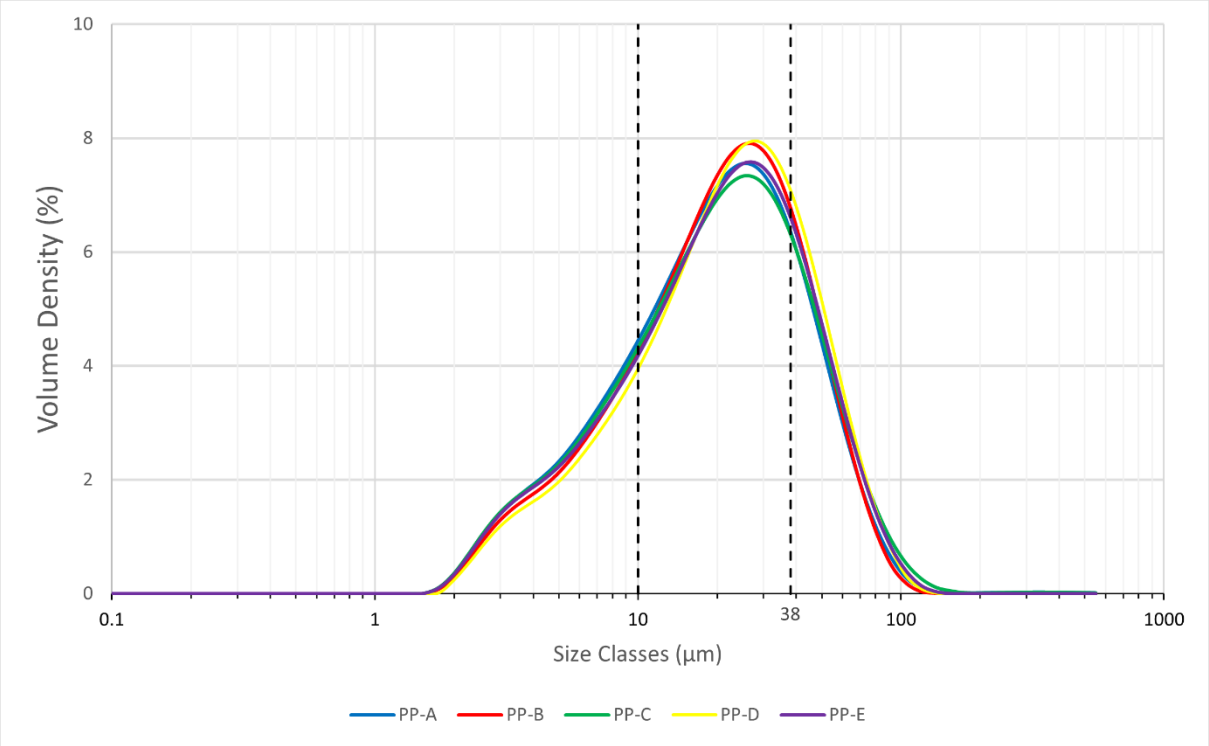

Figure 11: PSD of the L-fraction after filtration with highlighted target size range of 10 – 38 µm (n=5).

The RSD values (Figure 12A) can all be classified as relatively low (D10=4.54%; D50=3.51%; D90=2.69%). The uniformity value can also be considered low with a mean of 0.69 and a RSD of 5.21% (Figure 12B). This data indicates a high degree of reproducibility for the filtration of the L-fraction.

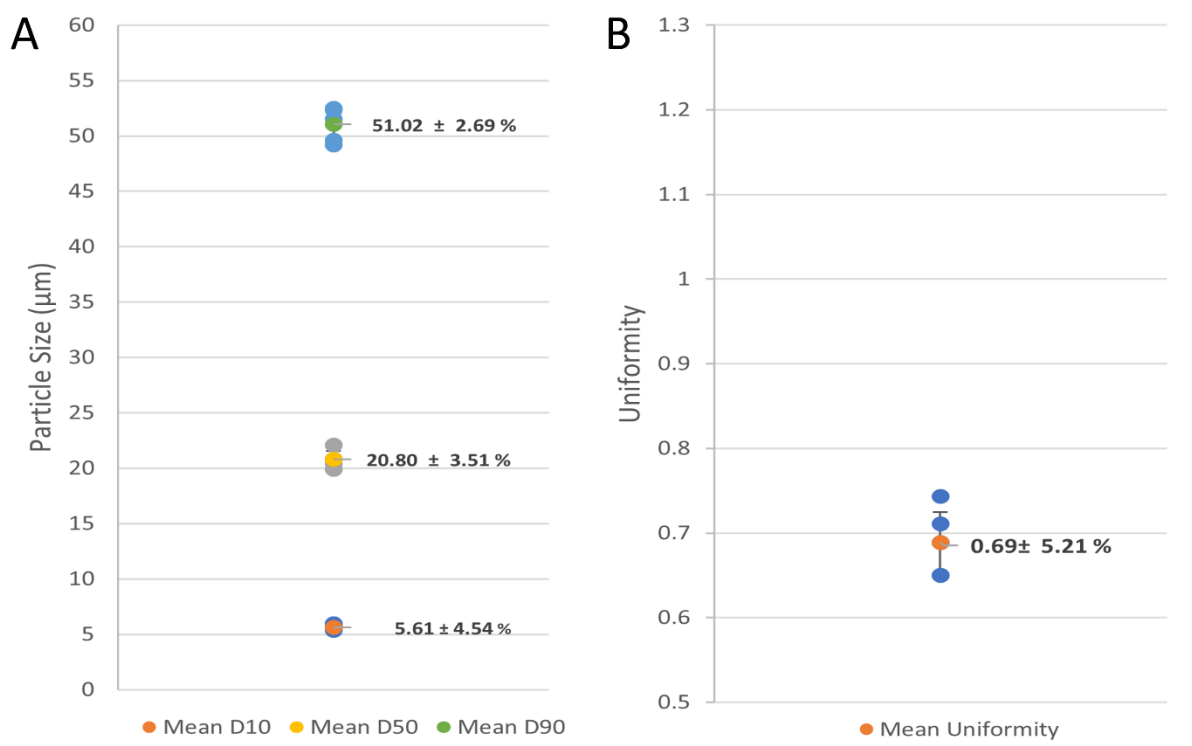

Figure 12: A) D10, D50 and D90 percentiles and B) uniformity data for the L fraction after filtration.

It should be noted however, that there are strong similarities in the PSD of the filtered L-fraction (Figure 11) and the LMS-fraction (Figure 9). A possible reason for this could be a clogging of the filter in the first filtration step, indicating that a large part of the LMS-fraction was not efficiently separated. This observation is further backed when comparing the percentiles of the L-fraction to the LMS-fraction, which also exhibit a high degree of similarity (Figure 13).

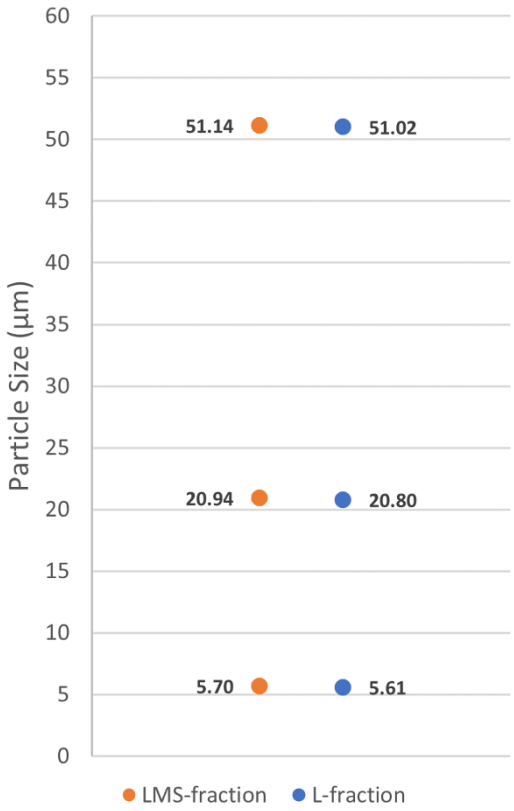

Figure 13: Comparison of mean D10-, D50- and D90-values of the LMS-fraction and the L-fraction after filtration.

To further investigate the reproducibility and efficiency of the filtration process, future studies could investigate methods to inhibit filter clogging and particle agglomeration. For example, developing a method of keeping PP particles in suspension and preventing them from agglomerating would likely result in a more consistent filtration process and better size separation.

3.2.2.2. Centrifugation

Centrifugation was the critical step in adjusting the PSD of the final L- and M-fractions to the desired size ranges. The fractions resulting from filtration were centrifuged in 2 main steps to remove unwanted particles.

The PSD of the L-fraction (Figure 14) shows a lower presence of smaller particles when compared to the original LMS-fraction (Figure 9). The peak of both PSD curves is roughly in the same size range, which could indicate that the size separation was more effective in removing unwanted smaller particles than it was for removing larger particles. The peak even shifted a little towards larger sizes, which could be because the larger particles had a greater relative contribution to the sample volume. Nonetheless, the peak of the curves is still below the 38 µm range, indicating that a

large part of the particles is indeed in the desired size range. Overall, the PSD of the L-fraction appears to be reproducible across multiple runs, suggesting that the centrifugation process was consistent.

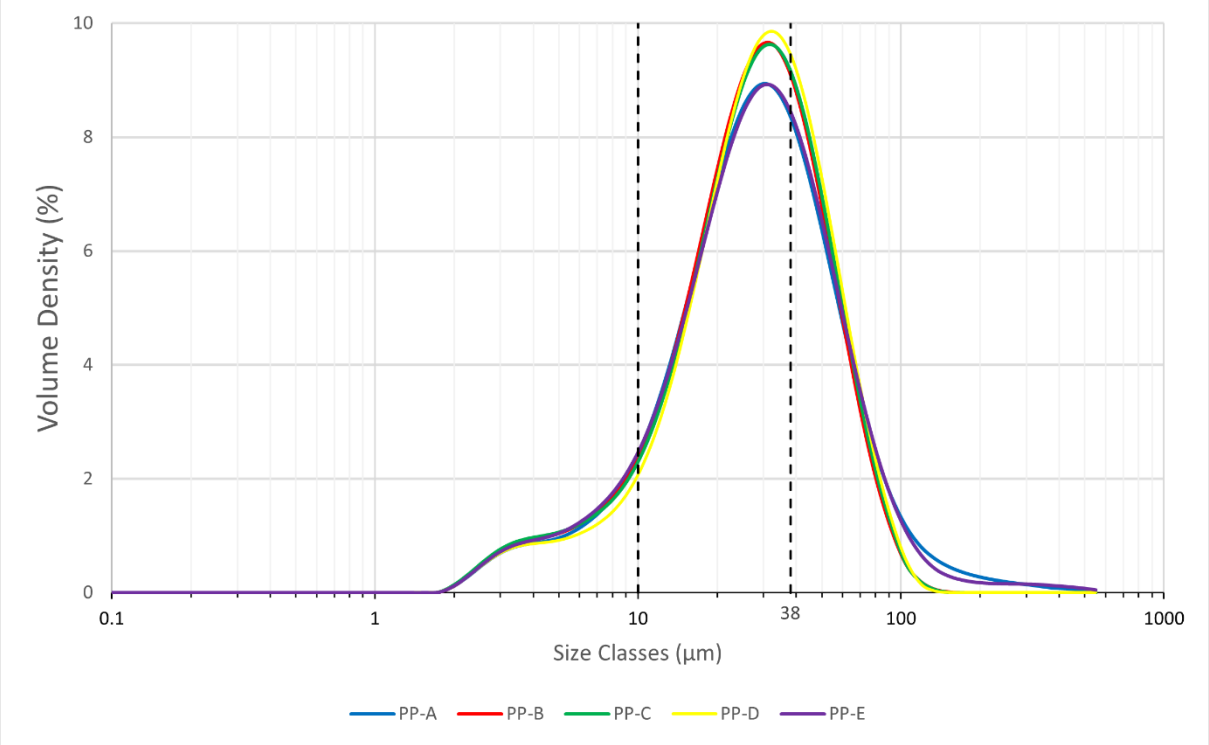

Figure 14: PSD of the L-fraction after centrifugation with highlighted target size range of 10 – 38 µm (n=5).

The comparatively low RSD values in the percentiles of the L-fraction (Figure 15A) also indicate good reproducibility across all 5 replicates. The RSD of the uniformity is higher than that of the filtered L-fraction, but the mean uniformity can still be considered low (Figure 15B). The yield exhibits high degree of variability in the L-fraction with an RSD of 26.99% (Figure 15C). One possible explanation is a combination of factors, including the previously mentioned gravimetric yield measurement, the error of the large number of manual steps that were necessary during the centrifugation process or simply because of the variation in the yield of the LMS-fraction. The mean total yield of 3.32 mg (0.017%) is also very low when the approximately 20 g of starting material are considered.

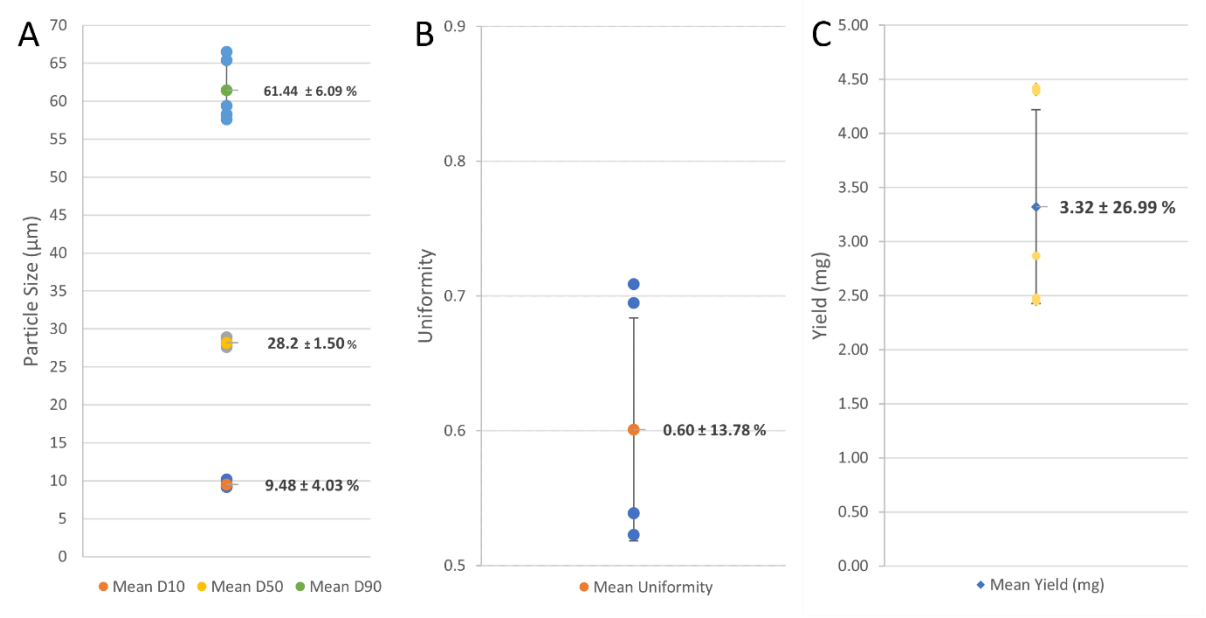

Figure 15: Reproducibility data of the L-fraction after centrifugation (n=5): A) D10, D50, and D90 percentiles including mean values ± RSD B) Uniformity of the PSD including the mean value ± RSD. C) Yield in mg including the mean value ± RSD.

In conclusion, the data indicates that the centrifugation process results in a reproducible L-fraction. The remaining concern is the low yield for the L-fraction. Because of this, future studies should investigate methods to increase the yield, for example by reusing the discarded fractions and further processing them to extract larger amounts of the desired particles or by increasing the efficiency of the milling process.

3.2.2.3. Medium exchange

For better cell culture compatibility, the dispersant was changed from ethanol to glycerol. This was done by drying the particles after the centrifugation to determine their yield, and subsequent resuspension in an ethanol and glycerol mixture. Finally, the ethanol was removed by evaporation. After the dispersant change was completed the PSDs of the samples were measured. In addition, the particle count was evaluated via counting under the microscope and with an automated cell counter.

The PSD of the L-fraction after the dispersant exchange (Figure 16) appears to be comparable to that of the L-fraction in EtOH. Additionally, it is worth noting that the 5 replicates within this fraction show no significant variation and thus can be considered reproducible.

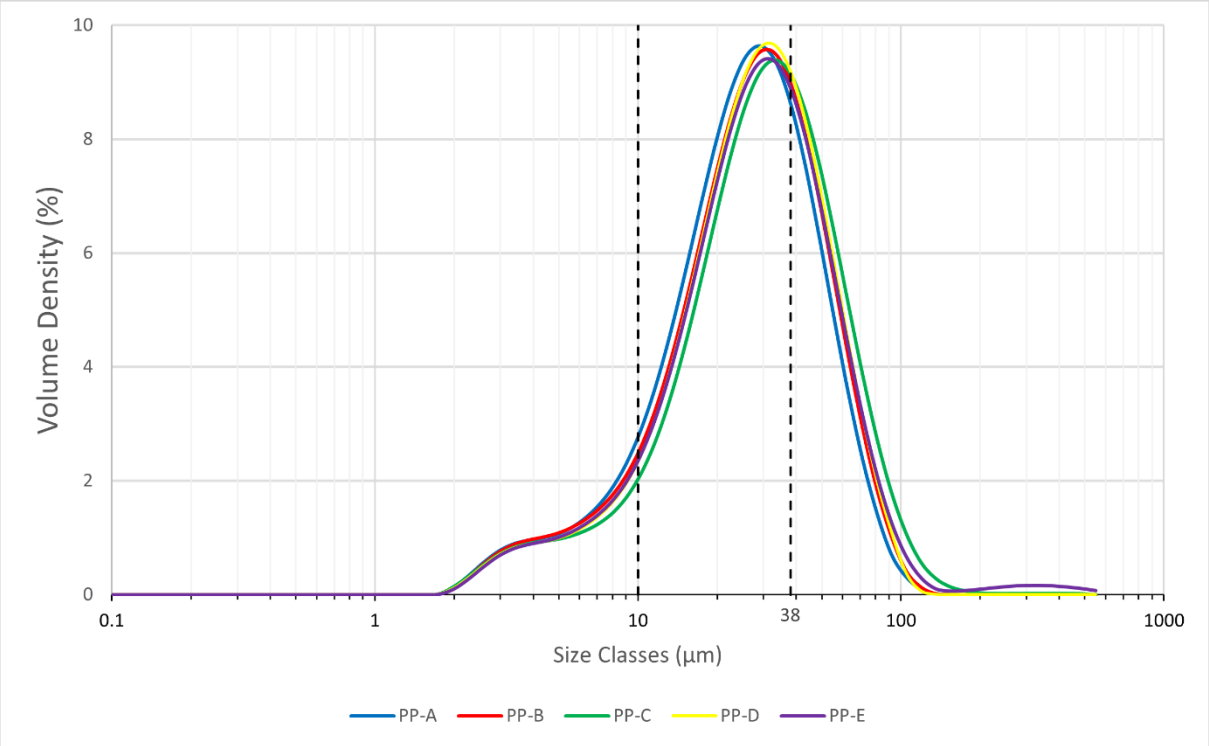

Figure 16: PSD of the centrifuged L-fraction in glycerin with highlighted target size range of 10 – 38 µm (n=5).

Comparing the percentiles of the L-fraction in glycerol and in ethanol (Figure 17A), it can be noted that they are relatively similar. Both the means and the RSDs seem to be in the same range, except for the RSD of D50, which is 4.91% for glycerol and 1.50% for EtOH. This confirms what was previously observed in the PSD. Looking at the uniformity-value (Figure 17B), it is also comparatively low with a mean of 0.57 and an RSD of 8.11%, considering that this is the last step in a long process where many cumulative errors are possible.

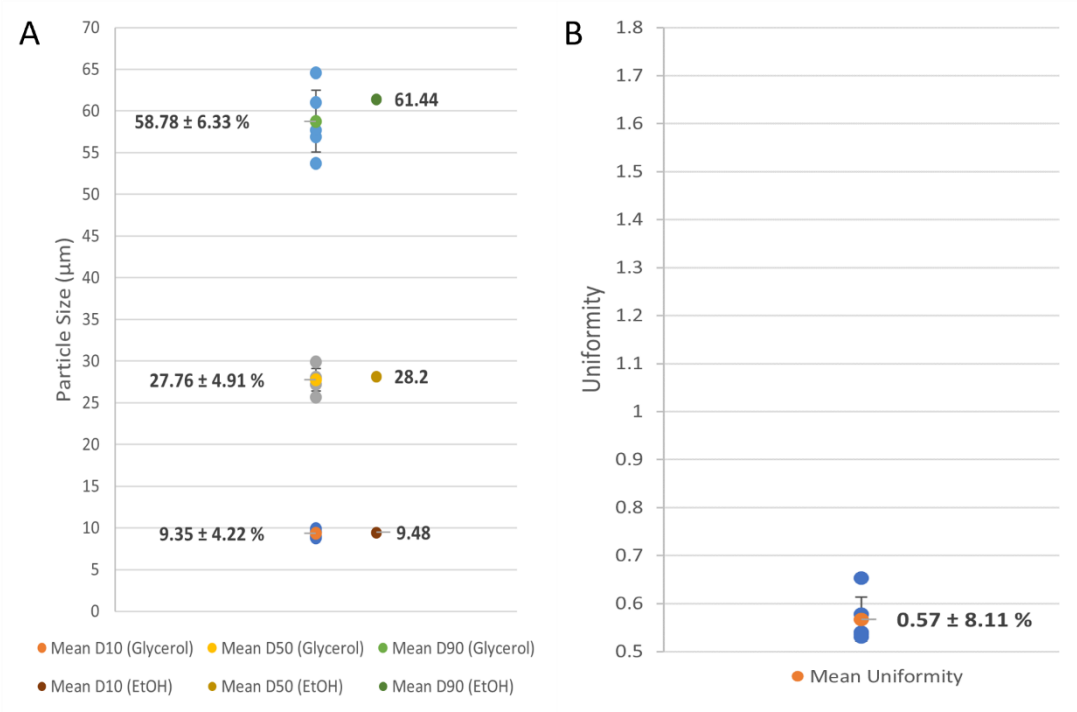

Figure 17: Reproducibility data of the L-fraction after the medium exchange (n=5): A) D10, D50, and D90 percentiles of the L-fraction including mean values ± RSD and mean percentiles of the L-fraction in EtOH B) Mean uniformity ± RSD.

When looking at the manual particle counts (Table 3), it can be noticed that the calculated concentration for each sample is in the same order of magnitude. The mean is 1,584,000 particles/mL and the RSD is 17.56%. In contrast to the previously determined RSDs for the yield after the sieving and centrifugation steps, this value is relatively low and thus shows a better reproducibility.

Table 3: Manually and automatically counted particle concentrations of the L-fraction of samples PP-A - E in particles/mL including mean values and RSD (%).

Method	PP-A	PP-B	PP-C	PP-D	PP-E	Mean	RSD
Manual	1,600,000	1,450,000	2,070,000	1,220,000	1,580,000	1,584,000	17.56%
Automatic	665,000	3,070,000	4,480,000	1,160,000	1,150,000	2,105,000	68.68%

On the other hand, the automatically counted concentrations exhibit a much larger RSD of 68.68% and display some irregularities. Samples PP-D and PP-E are in similar ranges, but the value for sample PP-A is lower than the manually counted concentration while PP-B and PP-C are approximately twice as high. The significance of this data is also limited because the automated count was performed only once per sample, whereas each sample was counted 8 times under the microscope. In addition, the instrument used was not designed to count plastic particles and was limited to counting particles > 5 µm. Therefore, only the concentrations from the manual count should be accepted.

Overall, the final L-fraction shows a high degree of reproducibility, indicating that the method is reliable and consistent in producing particles in the size range of 10-38 µm. Given the more consistent and reproducible results obtained with manual particle counting, this method may be more reliable for accurately determining the concentration of samples not only at the last stage of the process but also after the milling and centrifugation steps. Future studies could investigate the possibility of applying this method for determining particle concentrations.

3.2.3. Reproducibility of the M-fraction

3.2.3.1. Filtration

After the initial filtration step that separated the L-fraction from the LMS-fraction, a second filtration step was performed using a 0.8 µm filter. The material that remained on top of this filter was resuspended, which resulted in the M-fraction.

In the PSD of the M-fraction shown in Figure 18, only in samples PP-C and PP-E a relevant shift in the peak towards smaller particle sizes can be observed, indicating that the filtration influenced the particle separation to some extent in the wanted direction. Interestingly, these are also the samples that had the highest yields after the sieving. The PSD also shows that particles smaller than 1 µm were present in 4 out of 5 samples. This indicates that the production of small amounts of nanoparticles could be realized with this method. A possible explanation for why these particles were not detected in the LMS fraction may be that their concentration was too low, and they were overshadowed before by a much larger number of large particles. In contrast to the L- fraction, the M-fraction also has noticeable variation in the PSD, mainly in the larger particle sizes.

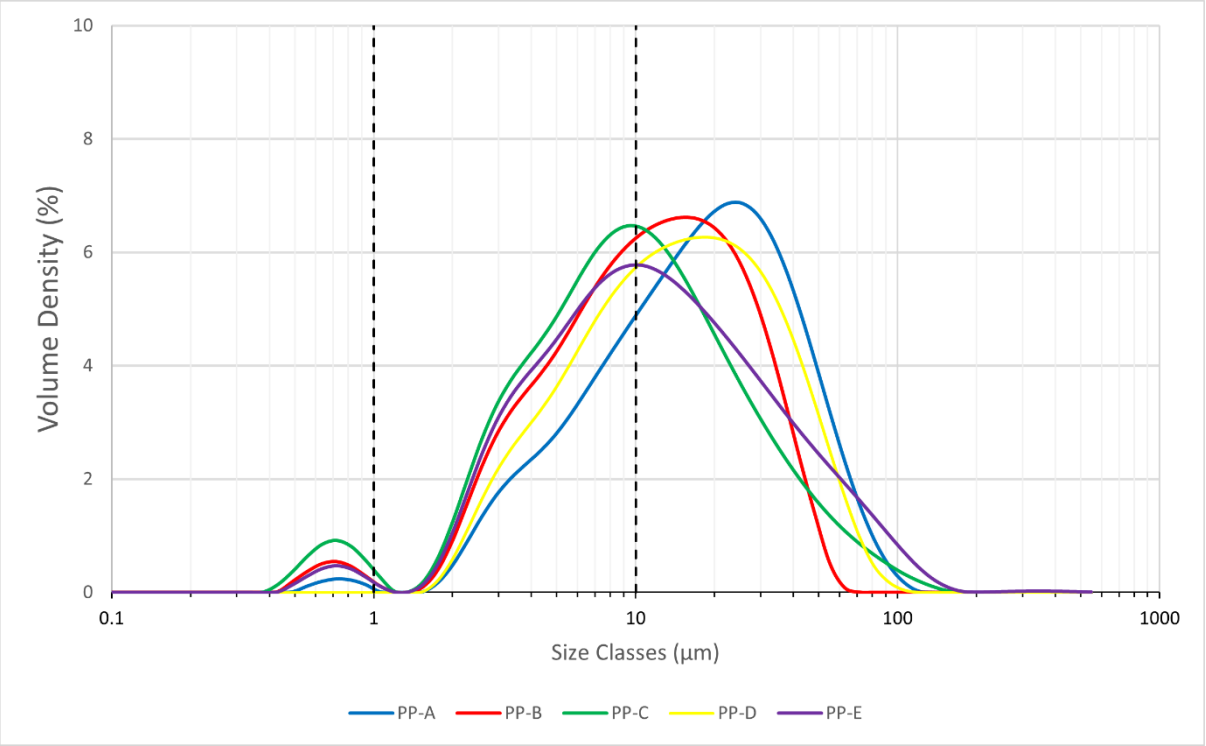

Figure 18: PSD of the M-fraction after filtration with highlighted target size range of 1 – 10 µm (n=5).

The differences shown in the PSD are further supported when examining the percentile and uniformity data of the curves shown in Figure 19. In contrast to the relatively low values the L-fraction had, the M-fraction exhibits higher RSD values (D10=16.27%; D50=21.64%; D90=17.48%) and a higher uniformity mean value of 0.91 with a RSD of 20.50%. These results suggest that the M-fraction has a wider range of particle sizes, with a less uniform distribution, compared to the L-fraction and thus these results cannot be considered reproducible.

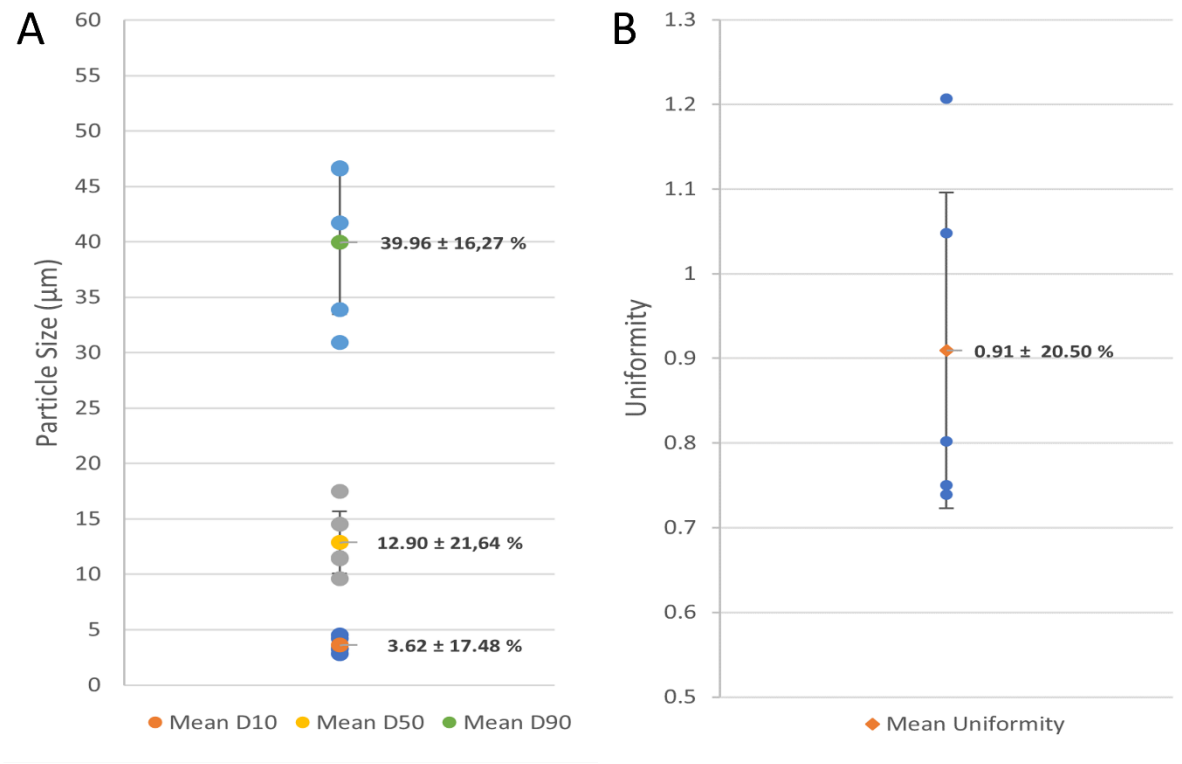

Figure 19: A) D10, D50 and D90 percentiles and B) uniformity data for the M-fraction after filtration.

Nevertheless, the separation succeeded at least to some extent. However, smaller particles below 1 µm were also contained in the M-fraction, which indicates incomplete separation during the second filtration step. This could also be caused by clogging of the filter and subsequent agglomeration of these small particles. As with the L-fraction, a possible way of inhibiting the filter clogging and agglomeration should be investigated in order to develop a reproducible filtration method for the M-fraction.

3.2.3.2. Centrifugation

As with the centrifugation of the L-fraction, the filtered M-fraction was processed in 2 centrifugation cycles to refine the product and remove particles outside the desired range.

The PSD of the M-fraction (Figure 20) seems to have more variation in comparison to the L-fraction. For example, in samples B and E there are still nanoparticles present in contrast to rest of the replicates which did not contain particles below 1 µm. In sample D, a tailing of the curve can be observed in the larger size ranges. This could be due to agglomeration of the particles or, for example, larger dust particles that contaminated the sample prior to the measurement. Overall, when disregarding the previously mentioned nanoparticles and the tailing in sample PP-D, the PSD of the M-fraction could be considered reproducible, especially when it is compared to the M-

fraction after filtration (Figure 18) and when the variation of the samples before the centrifugation is taken into account.

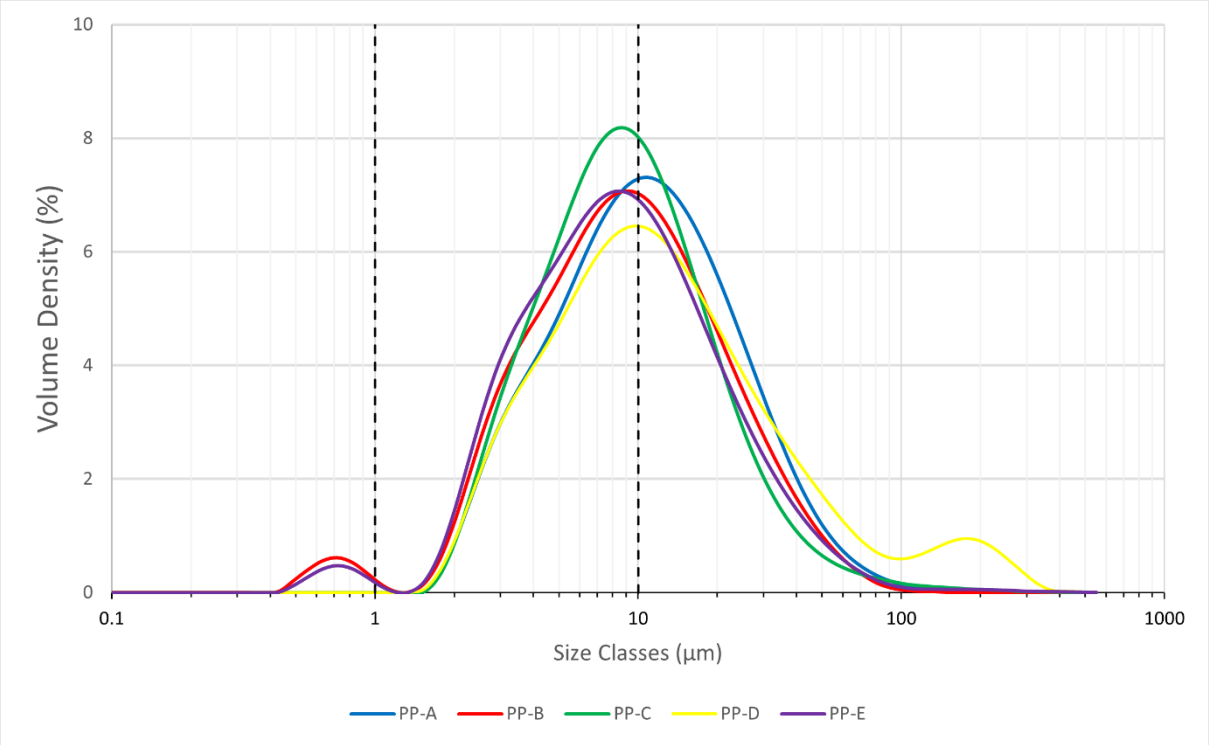

Figure 20: PSD of the M-fraction after centrifugation with highlighted target size range of 1 – 10 µm (n=5).

The D10 and D50 percentiles of the M-fraction (Figure 21A) have a much lower RSD, when compared to filtered M-fraction. This indicates a certain degree of reproducibility in these size ranges. In the D90 percentile, the previously mentioned outlier in the larger size ranges (PP-D) can be noticed. This also has an impact on the mean RSD values of the D90 percentile and the mean uniformity values and thus the reproducibility. However, if the mean and RSD are calculated without the outlier (PP-D), the mean D90 value changes to 26.65 µm with an RSD of only 7.92%. Based on these new values, the centrifugation of the M-fraction could be called reproducible.

As with the L-fraction yield is highly variable with an RSD of 33.59% (Figure 21C) and extremely low (0.91 mg; 0.0045%). The main reason for this is probably the low yield in the LMS-fraction and the material loss during the filtration and centrifugation.

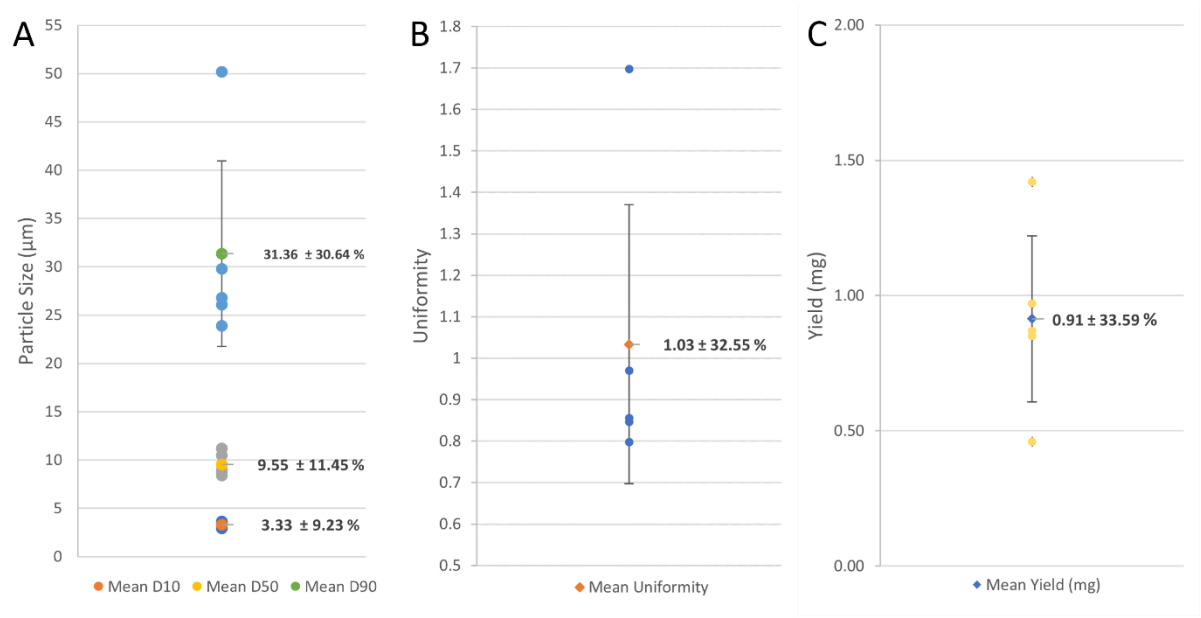

Figure 21: Reproducibility data of the M-fraction after centrifugation (n=5): A) D10, D50, and D90 percentiles including mean values ± RSD B) Uniformity of the PSD including the mean value ± RSD. C) Yield in mg including the mean value ± RSD.

3.2.3.3. Medium exchange

The medium exchange for the M-fraction was performed in the same way as for the L-fraction. After completion of the process, the particle concentration was determined only *via* manual particle counting. Automated counting, as with the L-fraction, was not possible, due to the counter's ability to count only particles > 5 µm.

The PSD of the M-fraction (Figure 22) shows more variation within its 5 replicates, when compared to the L-fraction and appears to be slightly different from the PSD of the M-fraction in EtOH (Figure 20). Furthermore, there are nanoparticles visible in sample PP-B.

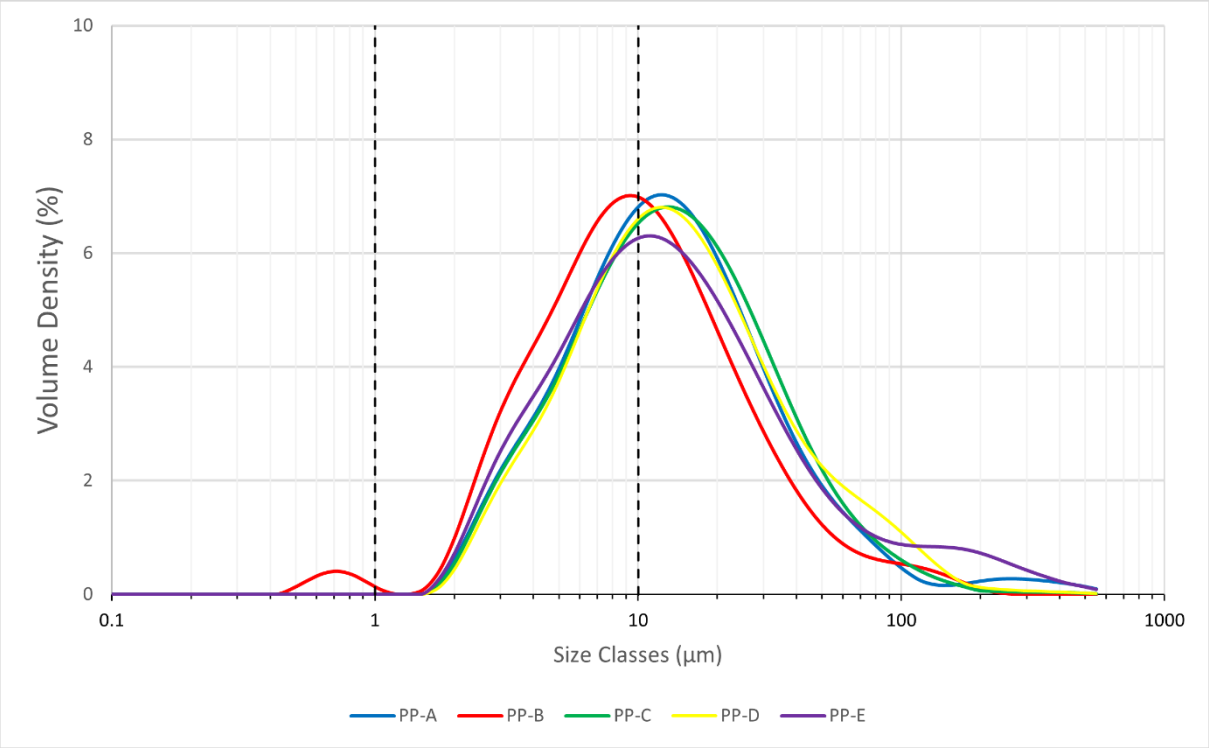

Figure 22: PSD of the centrifuged M-fraction in glycerin with highlighted target size range of 1 – 10 µm (n=5).

When looking at the percentiles, some differences compared to the EtOH sample can be observed (Figure 23A). On the one hand, the outlier that was visible after the centrifugation is no longer present in this sample, which reduces the RSD value to some extent, but it still appears to be relatively high. On the other hand, the mean D90 value is now much higher in the glycerol sample, which increased from 31.36 µm (EtOH) to 45.36 µm (glycerol). A reason for this probably lies in the medium exchange method. Presumably, the complete evaporation of the EtOH for the determination of the yield leads to an agglomeration of the particles, which can then no longer be completely redispersed by the subsequent addition of EtOH and heated glycerol. Since this is not observed in the L-fraction, it could be assumed that only smaller particles are affected by this. To confirm this, the samples would have to be examined by electron microscopy or similar methods. In addition, the PSDs of the M-fraction exhibit a relatively high uniformity mean and a high RSD, which shows a lack of reproducibility and an insufficient resuspension after the medium was changed.

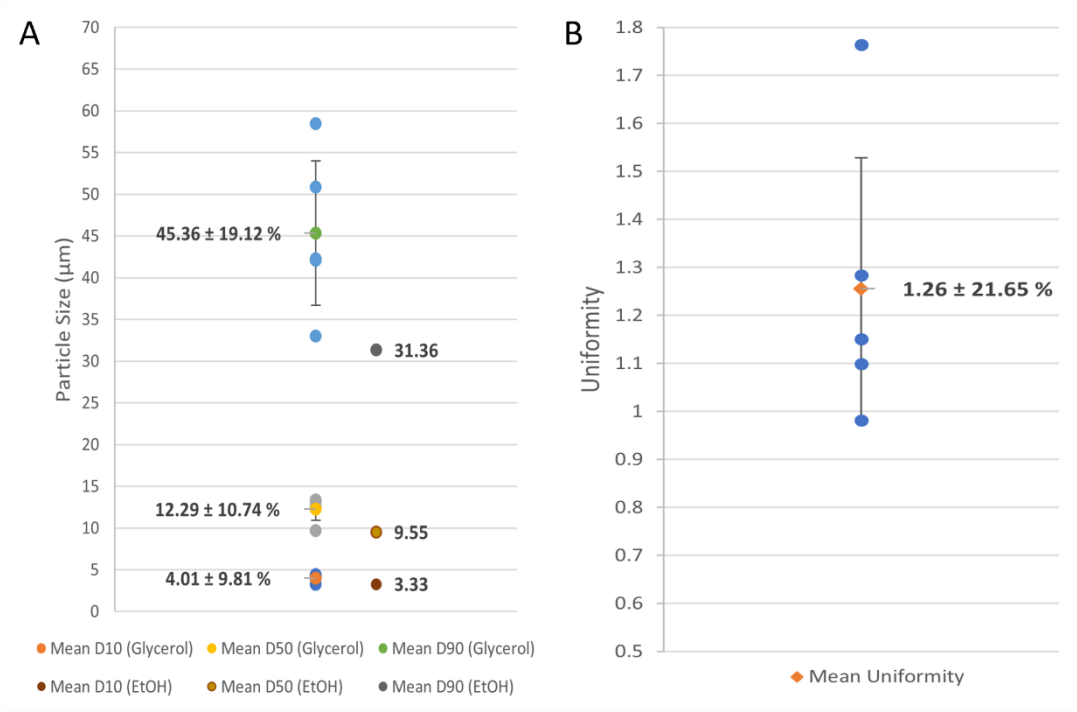

Figure 23: Reproducibility data of the M-fraction after the medium exchange (n=5): A) D10, D50, and D90 percentiles of the M-fraction including mean values ± RSD and mean percentiles of the M-fraction in EtOH B) Mean uniformity ± RSD.

Upon looking at the particle concentrations of the M-fraction in Table 4, it becomes apparent that the mean particle count is approximately twice as high as that of the L-fraction. Nevertheless, there is a higher RSD, indicating a greater degree of variability within these samples. A possible explanation for these irregularities could lie in the small particle sizes. It could be that particularly small particles were either not recognized as such by the operator and therefore not counted, or that several small particles agglomerated and were counted as only 1 particle.

Table 4: Manually counted particle concentrations of the M-fraction of samples PP-A - E in particles/mL including mean values and RSD (%).

Method	PP-A	PP-B	PP-C	PP-D	PP-E	Mean	RSD
Manual	1,310,000	2,640,000	3,610,000	4,580,000	3,790,000	3,186,000	35.25%

Overall, the medium exchange step did not yield sufficiently reproducible results for the M-fraction. Further studies are required to investigate the source of variability, for example by using electron microscopes to gain additional information on the behavior of the particles in glycerol and possibly confirm the agglomeration of the particles. In addition, the medium exchange process could be revised in order to achieve better reproducible results. This could involve optimizing the resuspension of the particles or modifying the medium exchange technique as a whole.

3.3. Reproducibility of the NIPS Procedure

Because of the very low quantities of PP particles that the mechanical grinding process yielded, an alternative production method was explored. This was particularly important for the production of nanoparticles. A non-solvent induced phase separation (NIPS) technique was used, which involves considerably fewer work steps and is generally expected to yield a larger amount of particles, in contrast to the milling process. To investigate the feasibility and reproducibility of this technique, a preliminary study with 8 replicates was conducted. At the end of production, the PSD of all 8 samples was measured and yields were determined for samples NIPS-PP-4 and NIPS-PP-5 (combined batches) and samples NIPS-PP-6 – 8 (individually). For samples NIPS-PP-1 – 3 the yield could not be determined because they were used for early size separation experiments.

The PSD curves (Figure 24) of all eight replicates show somewhat similar distribution characteristics, with a peak in the nano size range and a broader distribution in the micron size range up to 100 µm. The peaks, however, also exhibit variations in height, indicating differences in the particle volume density. This variability becomes more apparent when observing the D10, D50 and D90 percentiles of these samples

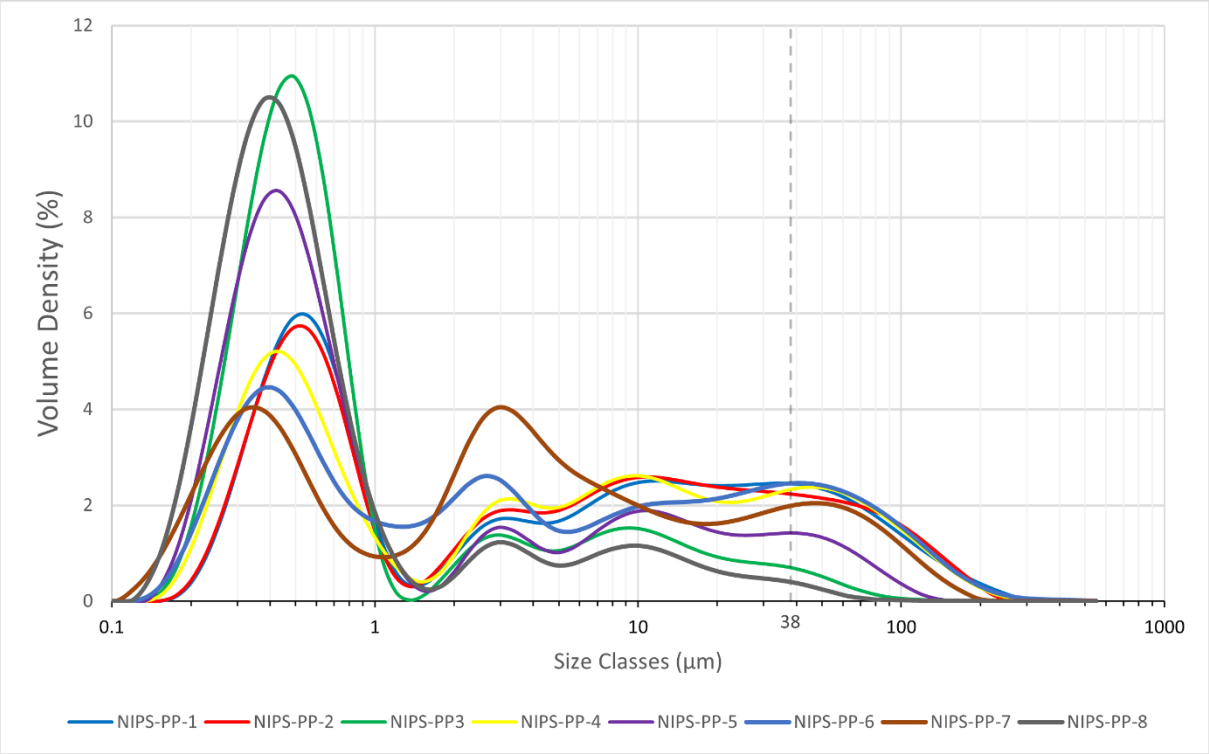

Figure 24: PSD of PP-particles produced using the NIPS method (n=8).

The percentiles all exhibit a relatively high variability (Figure 25). The D10 and D50 percentiles showed relatively low mean values (0.312 µm and 2.62 µm respectively), indicating that a larger percentage of the particles are indeed nano sized. In contrast, the mean value of the D90 percentile (43.42 µm) is comparatively high and can be compared to the D90 value of the LMS-fraction after the mechanical grinding. A possible reason for this lies in the step where the PP solution is added to the non-solvent. It is possible that during the production process some of the solution remained on the wall of the beaker. This could have prevented the dissolved PP from undergoing NIPS and instead caused the formation of larger particles upon cooling on the beaker walls. These larger particles could have been subsequently washed into the suspension and thus contributed to the above-mentioned observations. Moreover, all percentiles exhibit relatively high RSD values, indicating that, without modifications and further processing of the particles, this method is not reproducible.

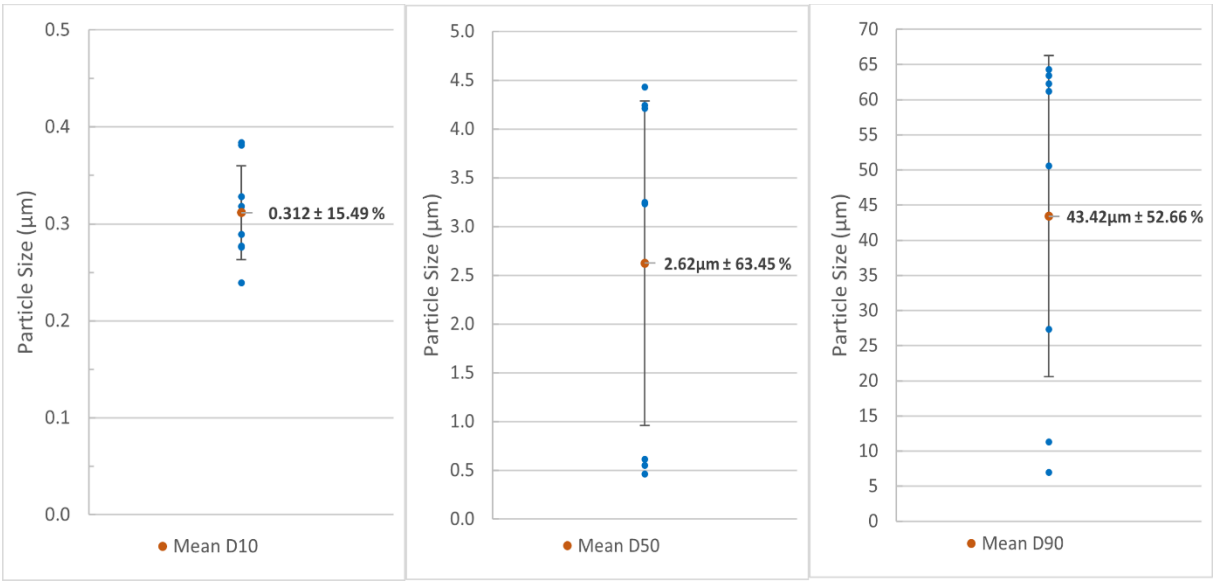

Figure 25: D10, D50 and D90 values including mean values ± RSD (n=8).

Despite this lack of adequate reproducibility, a great advantage of this method is the high yield that can be achieved. As shown in Figure 26, the mean yield of this method (n=4) is 89.85% (245.74 mg) and has a low RSD value of 2.42%. This indicates that this method can consistently yield a large amount of PP particles. However, it has to be noted that only 4 replicates were made and thus the statistical significance of the data is somewhat limited.

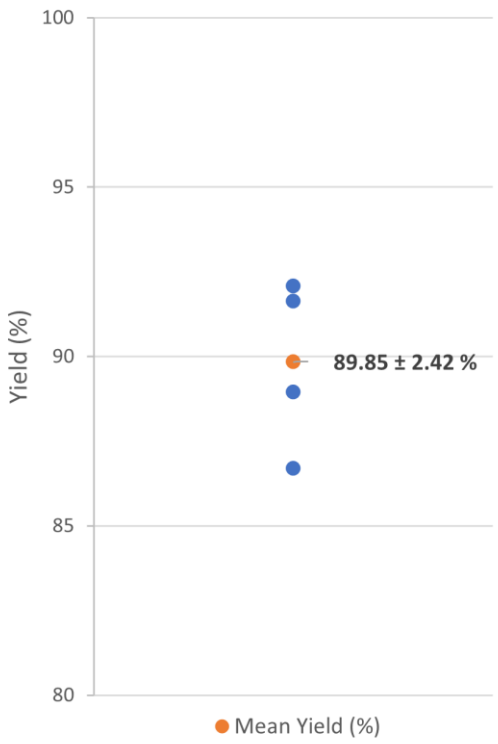

Figure 26: Yield Data of the NIPS method including mean value ± RSD (n=4).

Overall, those findings suggest that it is possible to produce a large amount of PP particles and in particular nanometer-sized particles. However, the data also indicated a lack of reproducibility, which could be due to the inability to precisely control production parameters such as the manual addition of the PP solution to the non-solvent, which could give rise to human error. In addition, it must be noted that particles produced by NIPS could result in a different surface structure and shape compared to those produced via mechanical grinding and the ones present in nature. Furthermore, particles in this size range agglomerate too during the dispersant exchange, like it was observed in the mechanical grinding process and thus this needs to be considered in future experiments.

4. Conclusion

In order to determine the best method for producing test material, it is important to compare the strengths and weaknesses of each technique. It is important to note that only the LMS-fraction can be adequately compared to the particles produced via NIPS, since at this point no size separation was performed.

The main reason why a mechanical grinding method was applied, was that the resulting particles are likely to be similar in shape and surface morphology to those

found in the oceans and thus their behavior in toxicity experiments is expected to be more realistic. The particles produced via the NIPS method on the other hand are likely to be of a rather spherical shape and differ in their surface morphology from the milled particles. To confirm this, additional investigations of the exact surface morphology of both kinds of particles via electron microscopy are necessary. However, while the NIPS method may not produce particles with the desired morphology, it does have the advantage of forming a large number of nanoparticles which could not be produced by grinding. The relative yield of both methods is also a factor that needs to be considered. While the mean yield for the LMS-fraction is 0.38% and exhibits a relatively high RSD of 50.57%, the NIPS method yielded a mean of 89.85% with a RSD of only 2.42%.

The production of the LMS fraction can be considered reproducible. In contrast, the particles resulting from the NIPS method were deemed not reproducible, since their PSD and their percentiles showed too much variation. The production time is also an important factor. Manufacturing the LMS fraction, the PP needs to be pre-treated, frozen and then milled, which amounts to approximately 16 hours of total time needed. The NIPS method on the other hand only takes around 4 hours per batch.

It can be concluded that both methods have their respective strengths and weaknesses. Since the surface morphology is a very important aspect of these reference particles the mechanical grinding should be kept as the main method of production for particles > 10 µm. However, the method should be optimized in terms of an increased yield and production time. To produce particles in the size range of 1–10 µm, the protocol for the M-fraction should be revised in order to achieve reproducible results and a higher yield. In addition, if this approach does not produce the desired results, possibilities for a completely new production method could be explored. The NIPS method is a particularly interesting method for producing NPs, but it should also be optimized to achieve more reproducible results and efforts should be made to further refine the NP fraction and to remove unwanted larger particles. In addition, future investigations of the shape and possible agglomeration of the particles should be made *via* electron microscopy.

5. Outlook

Based on the results of this thesis, one of the main focus points of future studies should be finding ways of increasing the yield of the milled PP-particles. One simple way to achieve this could be by reusing the discarded material and repeating key production

steps such as the centrifugation or the sieving. Sieving appears to be step that limits the yield the most. A reason for this could be aggregation on top of the sieves severely inhibiting a passing of the particles. A way to inhibit this could be by modifying the sieve tower by adding a nozzle and outlet to allow a continuous flow of EtOH through the sieves. This could greatly increase the yield of the LMS-fraction. However, this would also lead to higher equipment and material costs and probably increase the overall time for production as well since of the greatly increased use of EtOH. The use of a surfactant such as Tween® could also be a possibility to inhibit aggregation on the sieves, however this would come with the problem of removing the added surfactant at a later stage in the process. A way to do this could be by filtering and washing the final product prior to the medium change. If a substantial yield increase is achieved, the filtration and centrifugation steps would need to be modified and scaled up in order to maintain product quality. For the filtration a possible approach for this would be to find a way to inhibit filter clogging. A somewhat simple solution to this problem would be to use multiple filters and to filter the LMS-fraction in small increments. Another way could be by implementing a way of keeping the particles in suspension, possibly by stirring or air suspension. For the centrifugation, a use of larger centrifuge tubes could be sufficient.

Another major concern is the lack of reproducibility of the M-fraction. Hereby, the agglomeration of the small PP-particles during the filtration and centrifugation is thought to be the main problem. A logical first step would be to confirm this assumption by using an electron microscopy method. If the agglomeration is confirmed, methods to prevent this would need to be investigated. As with the yield increase the use of Tween® could prove effective. However, this would come with the previously mentioned problem of removing it at the end of the process. Together with the previously mentioned approaches to improve the filtration this could lead to a more reproducible M-fraction process.

If a reproducible M-fraction is still not achieved after optimization, other production methods would need to be considered. Perhaps the NIPS method could be used to also produce particles in this size range. However, this comes with the disadvantage of the unfavorable morphology of the particles. A completely different method, although very unlikely and expensive, could be to try a tangential flow filtration approach to efficiently separate the MPs after the sieving. The feasibility of this approach would need to be investigated.

Finally, the size separation of the NPs, mainly the removal of the unwanted particles > 1 µm, would need to be performed. It is assumed that, as with the M-fraction, the smaller particles in the sample would likely aggregate during size separation steps. As mentioned before, a solution for this could be the use of a surfactant. Another possibility would be to centrifuge the sample in multiple small increments to decrease the concentration of the particles and thereby lowering the chances of aggregation.

List of Figures

List of Tables

References

[1] R. Geyer, J. R. Jambeck, and K. L. Law, "Production, use, and fate of all plastics ever made," *Sci Adv*, vol. 3, no. 7, 2017, doi: 10.1126/sciadv.1700782.

[2] PlasticsEurope, "Plastics – the Facts 2020. Brussels," *Plastics Europe: Association of Plastics Manufacturers*, 2020.

[3] J. Zheng and S. Suh, "Strategies to reduce the global carbon footprint of plastics," *Nature Climate Change*, vol. 9, no. 5. 2019. doi: 10.1038/s41558-019-0459-z.

[4] A. L. Andrady and M. A. Neal, "Applications and societal benefits of plastics," *Philosophical Transactions of the Royal Society B: Biological Sciences*, vol. 364, no. 1526, 2009, doi: 10.1098/rstb.2008.0304.

[5] PlascticsEurope, "Plastics-the Facts 2021 An analysis of European plastics production, demand and waste data."

[6] A. Chamas *et al.*, "Degradation Rates of Plastics in the Environment," *ACS Sustain Chem Eng*, vol. 8, no. 9, 2020, doi: 10.1021/acssuschemeng.9b06635.

[7] Hisham A. Maddah, "Polypropylene as a Promising Plastic: A Review," *American Journal of Polymer Science*, 2016, doi: 10.5923/j.ajps.20160601.01.

[8] C. Campanale, C. Massarelli, I. Savino, V. Locaputo, and V. F. Uricchio, "A detailed review study on potential effects of microplastics and additives of concern on human health," *International Journal of Environmental Research and Public Health*, vol. 17, no. 4. 2020. doi: 10.3390/ijerph17041212.

[9] H. Alhazmi, F. H. Almansour, and Z. Aldhafeeri, "Plastic waste management: A review of existing life cycle assessment studies," *Sustainability (Switzerland)*, vol. 13, no. 10. 2021. doi: 10.3390/su13105340.

[10] M. Eriksen *et al.*, "Plastic Pollution in the World's Oceans: More than 5 Trillion Plastic Pieces Weighing over 250,000 Tons Afloat at Sea," *PLoS One*, vol. 9, no. 12, 2014, doi: 10.1371/journal.pone.0111913.

[11] M. A. Browne *et al.*, "Accumulation of microplastic on shorelines woldwide: Sources and sinks," *Environ Sci Technol*, vol. 45, no. 21, 2011, doi: 10.1021/es201811s.

[12] J. Barrett *et al.*, "Microplastic Pollution in Deep-Sea Sediments From the Great Australian Bight," *Front Mar Sci*, vol. 7, 2020, doi: 10.3389/fmars.2020.576170.

[13] R. Dris, J. Gasperi, V. Rocher, M. Saad, N. Renault, and B. Tassin, "Microplastic contamination in an urban area: A case study in Greater Paris," *Environmental Chemistry*, vol. 12, no. 5, 2015, doi: 10.1071/EN14167.

[14] S. Allen *et al.*, "Atmospheric transport and deposition of microplastics in a remote mountain catchment," *Nat Geosci*, vol. 12, no. 5, 2019, doi: 10.1038/s41561-019-0335-5.

[15] A. Cincinelli *et al.*, "Microplastic in the surface waters of the Ross Sea (Antarctica): Occurrence, distribution and characterization by FTIR," *Chemosphere*, vol. 175, 2017, doi: 10.1016/j.chemosphere.2017.02.024.

[16] L. C. Jenner, J. M. Rotchell, R. T. Bennett, M. Cowen, V. Tentzeris, and L. R. Sadofsky, "Detection of microplastics in human lung tissue using μFTIR spectroscopy," *Science of the Total Environment*, vol. 831, 2022, doi: 10.1016/j.scitotenv.2022.154907.

[17] J. L. Pauly *et al.*, "Inhaled cellulosic and plastic fibers found in human lung tissue," *Cancer Epidemiology Biomarkers and Prevention*, vol. 7, no. 5, 1998.

[18] P. Schwabl *et al.*, "Detection of various microplastics in human stool: A prospective case series," *Ann Intern Med*, vol. 171, no. 7, 2019, doi: 10.7326/M19-0618.

[19] H. A. Leslie, M. J. M. van Velzen, S. H. Brandsma, A. D. Vethaak, J. J. Garcia-Vallejo, and M. H. Lamoree, "Discovery and quantification of plastic particle pollution in human blood," *Environ Int*, vol. 163, 2022, doi: 10.1016/j.envint.2022.107199.

[20] R. C. Thompson *et al.*, "Lost at Sea: Where Is All the Plastic?," *Science (1979)*, vol. 304, no. 5672, 2004, doi: 10.1126/science.1094559.

[21] E. R. Graham and J. T. Thompson, “Deposit- and suspension-feeding sea cucumbers (Echinodermata) ingest plastic fragments,” *J Exp Mar Biol Ecol*, vol. 368, no. 1, 2009, doi: 10.1016/j.jembe.2008.09.007.

[22] M. A. Browne, T. S. Galloway, and R. C. Thompson, “Spatial patterns of plastic debris along estuarine shorelines,” *Environ Sci Technol*, vol. 44, no. 9, 2010, doi: 10.1021/es903784e.

[23] M. Claessens, L. van Cauwenberghe, M. B. Vandegehuchte, and C. R. Janssen, “New techniques for the detection of microplastics in sediments and field collected organisms,” *Mar Pollut Bull*, vol. 70, no. 1–2, 2013, doi: 10.1016/j.marpolbul.2013.03.009.

[24] X. Z. Lim, “Microplastics are everywhere - but are they harmful?,” *Nature*, vol. 593, no. 7857. 2021. doi: 10.1038/d41586-021-01143-3.

[25] “NOAA. What are microplastics? National Ocean Service website,” *23*. https://oceanservice.noaa.gov/facts/microplastics.html (accessed Feb. 09, 2023).

[26] N. B. Hartmann *et al.*, “Are We Speaking the Same Language? Recommendations for a Definition and Categorization Framework for Plastic Debris,” *Environ Sci Technol*, vol. 53, no. 3, 2019, doi: 10.1021/acs.est.8b05297.

[27] S. Iwasaki, A. Isobe, S. Kako, K. Uchida, and T. Tokai, “Fate of microplastics and mesoplastics carried by surface currents and wind waves: A numerical model approach in the Sea of Japan,” *Mar Pollut Bull*, vol. 121, no. 1–2, 2017, doi: 10.1016/j.marpolbul.2017.05.057.

[28] O. S. Alimi, J. Farner Budarz, L. M. Hernandez, and N. Tufenkji, “Microplastics and Nanoplastics in Aquatic Environments: Aggregation, Deposition, and Enhanced Contaminant Transport,” *Environmental Science and Technology*, vol. 52, no. 4. 2018. doi: 10.1021/acs.est.7b05559.

[29] ISO, “ISO/TR 21960:2020(en) Plastics — Environmental aspects — State of knowledge and methodologies,” Feb. 2020. https://www.iso.org/obp/ui/#iso:std:72300:en (accessed Jun. 21, 2023).

[30] A. , K. D. Jemec Kokalj, “euon.echa.europa.eu.” https://euon.echa.europa.eu/nanopinion/-/blogs/are-nanoplastics-hazardous-the-way-forward-to-overcome-the-uncertainties-of-risk-

assessment#:~:text=Nanoplastics%20are%20solid%20particles%20of,nm%2C%20as%20for%20engineered%20nanomaterials. (accessed Jun. 21, 2023).

[31] C. L. Waller *et al.*, "Microplastics in the Antarctic marine system: An emerging area of research," *Science of the Total Environment*, vol. 598. 2017. doi: 10.1016/j.scitotenv.2017.03.283.

[32] M. Cole, P. Lindeque, C. Halsband, and T. S. Galloway, "Microplastics as contaminants in the marine environment: A review," *Marine Pollution Bulletin*, vol. 62, no. 12. 2011. doi: 10.1016/j.marpolbul.2011.09.025.

[33] L. S. Fendall and M. A. Sewell, "Contributing to marine pollution by washing your face: Microplastics in facial cleansers," *Mar Pollut Bull*, vol. 58, no. 8, 2009, doi: 10.1016/j.marpolbul.2009.04.025.

[34] M. Chang, "Reducing microplastics from facial exfoliating cleansers in wastewater through treatment versus consumer product decisions," *Mar Pollut Bull*, vol. 101, no. 1, 2015, doi: 10.1016/j.marpolbul.2015.10.074.

[35] M. R. Gregory, "Plastic scrubbers' in hand cleansers: A further (and minor) source for marine pollution identified," *Mar Pollut Bull*, vol. 32, no. 12, 1996, doi: 10.1016/S0025-326X(96)00047-1.

[36] A. L. Andrady, "Microplastics in the marine environment," *Marine Pollution Bulletin*, vol. 62, no. 8. 2011. doi: 10.1016/j.marpolbul.2011.05.030.

[37] A. L. Andrady *et al.*, "Oxidation and fragmentation of plastics in a changing environment; from UV-radiation to biological degradation," *Science of The Total Environment*, vol. 851, p. 158022, 2022, doi: https://doi.org/10.1016/j.scitotenv.2022.158022.

[38] A. K. Rodriguez, B. Mansoor, G. Ayoub, X. Colin, and A. A. Benzerga, "Effect of UV-aging on the mechanical and fracture behavior of low density polyethylene," *Polym Degrad Stab*, vol. 180, 2020, doi: 10.1016/j.polymdegradstab.2020.109185.

[39] D. K. A. Barnes, F. Galgani, R. C. Thompson, and M. Barlaz, "Accumulation and fragmentation of plastic debris in global environments," *Philosophical Transactions of the Royal Society B: Biological Sciences*, vol. 364, no. 1526, 2009, doi: 10.1098/rstb.2008.0205.

[40] J. Gigault, B. Pedrono, B. Maxit, and A. Ter Halle, “Marine plastic litter: The unanalyzed nano-fraction,” *Environ Sci Nano*, vol. 3, no. 2, 2016, doi: 10.1039/c6en00008h.

[41] S. Bahl, J. Dolma, J. J. Singh, and S. Sehgal, “Biodegradation of plastics: A state of the art review,” in *Materials Today: Proceedings*, 2020. doi: 10.1016/j.matpr.2020.06.096.

[42] A. Mateos-Cárdenas, J. O’Halloran, F. N. A. M. van Pelt, and M. A. K. Jansen, “Rapid fragmentation of microplastics by the freshwater amphipod Gammarus duebeni (Lillj.),” *Sci Rep*, vol. 10, no. 1, 2020, doi: 10.1038/s41598-020-69635-2.

[43] S. Kefer, O. Miesbauer, and H. C. Langowski, “Environmental microplastic particles vs. Engineered plastic microparticles—a comparative review,” *Polymers*, vol. 13, no. 17. 2021. doi: 10.3390/polym13172881.

[44] S. Karbalaei, P. Hanachi, T. R. Walker, and M. Cole, “Occurrence, sources, human health impacts and mitigation of microplastic pollution,” *Environmental Science and Pollution Research*, vol. 25, no. 36. 2018. doi: 10.1007/s11356-018-3508-7.

[45] P. L. Lenaker, A. K. Baldwin, S. R. Corsi, S. A. Mason, P. C. Reneau, and J. W. Scott, “Vertical Distribution of Microplastics in the Water Column and Surficial Sediment from the Milwaukee River Basin to Lake Michigan,” *Environ Sci Technol*, vol. 53, no. 21, 2019, doi: 10.1021/acs.est.9b03850.

[46] R. Dris, J. Gasperi, M. Saad, C. Mirande, and B. Tassin, “Synthetic fibers in atmospheric fallout: A source of microplastics in the environment?,” *Mar Pollut Bull*, vol. 104, no. 1–2, 2016, doi: 10.1016/j.marpolbul.2016.01.006.

[47] J. Gasperi *et al.*, “Microplastics in air: Are we breathing it in?,” *Current Opinion in Environmental Science and Health*, vol. 1. 2018. doi: 10.1016/j.coesh.2017.10.002.

[48] J. C. Prata, “Airborne microplastics: Consequences to human health?,” *Environmental Pollution*, vol. 234. 2018. doi: 10.1016/j.envpol.2017.11.043.

[49] K. Zhang, J. Su, X. Xiong, X. Wu, C. Wu, and J. Liu, “Microplastic pollution of lakeshore sediments from remote lakes in Tibet plateau, China,” *Environmental Pollution*, vol. 219, 2016, doi: 10.1016/j.envpol.2016.05.048.

[50] S. Allen, D. Allen, K. Moss, G. le Roux, V. R. Phoenix, and J. E. Sonke, “Examination of the ocean as a source for atmospheric microplastics,” *PLoS One*, vol. 15, no. 5, 2020, doi: 10.1371/journal.pone.0232746.

[51] E. Molina and S. Benedé, "Is There Evidence of Health Risks From Exposure to Micro- and Nanoplastics in Foods?," *Front Nutr*, vol. 9, 2022, doi: 10.3389/fnut.2022.910094.

[52] L. G. A. Barboza, A. Dick Vethaak, B. R. B. O. Lavorante, A. K. Lundebye, and L. Guilhermino, "Marine microplastic debris: An emerging issue for food security, food safety and human health," *Marine Pollution Bulletin*, vol. 133. 2018. doi: 10.1016/j.marpolbul.2018.05.047.

[53] E. Curren, C. P. Leaw, P. T. Lim, and S. C. Y. Leong, "Evidence of Marine Microplastics in Commercially Harvested Seafood," *Front Bioeng Biotechnol*, vol. 8, 2020, doi: 10.3389/fbioe.2020.562760.

[54] A. A. Koelmans, N. H. Mohamed Nor, E. Hermsen, M. Kooi, S. M. Mintenig, and J. De France, "Microplastics in freshwaters and drinking water: Critical review and assessment of data quality," *Water Research*, vol. 155. 2019. doi: 10.1016/j.watres.2019.02.054.

[55] J. Talvitie, A. Mikola, A. Koistinen, and O. Setälä, "Solutions to microplastic pollution – Removal of microplastics from wastewater effluent with advanced wastewater treatment technologies," *Water Res*, vol. 123, 2017, doi: 10.1016/j.watres.2017.07.005.

[56] A. A. de Souza Machado, W. Kloas, C. Zarfl, S. Hempel, and M. C. Rillig, "Microplastics as an emerging threat to terrestrial ecosystems," *Global Change Biology*, vol. 24, no. 4. 2018. doi: 10.1111/gcb.14020.

[57] M. Revel, A. Châtel, and C. Mouneyrac, "Micro(nano)plastics: A threat to human health?," *Current Opinion in Environmental Science and Health*, vol. 1. 2018. doi: 10.1016/j.coesh.2017.10.003.

[58] L. M. Hernandez, E. G. Xu, H. C. E. Larsson, R. Tahara, V. B. Maisuria, and N. Tufenkji, "Plastic Teabags Release Billions of Microparticles and Nanoparticles into Tea," *Environ Sci Technol*, vol. 53, no. 21, 2019, doi: 10.1021/acs.est.9b02540.

[59] R. Dris *et al.*, "A first overview of textile fibers, including microplastics, in indoor and outdoor environments," *Environmental Pollution*, vol. 221, 2017, doi: 10.1016/j.envpol.2016.12.013.

[60] R. Lehner, C. Weder, A. Petri-Fink, and B. Rothen-Rutishauser, "Emergence of Nanoplastic in the Environment and Possible Impact on Human Health," *Environmental Science and Technology*. 2019. doi: 10.1021/acs.est.8b05512.

[61] S. Rist, B. Carney Almroth, N. B. Hartmann, and T. M. Karlsson, "A critical perspective on early communications concerning human health aspects of microplastics," *Science of the Total Environment*, vol. 626. 2018. doi: 10.1016/j.scitotenv.2018.01.092.

[62] K. D. Cox, G. A. Covernton, H. L. Davies, J. F. Dower, F. Juanes, and S. E. Dudas, "Human Consumption of Microplastics," *Environ Sci Technol*, vol. 53, no. 12, 2019, doi: 10.1021/acs.est.9b01517.

[63] N. Hussain, V. Jaitley, and A. T. Florence, "Recent advances in the understanding of uptake of microparticulates across the gastrointestinal lymphatics," *Advanced Drug Delivery Reviews*, vol. 50, no. 1–2. 2001. doi: 10.1016/S0169-409X(01)00152-1.

[64] S. L. Wright and F. J. Kelly, "Plastic and Human Health: A Micro Issue?," *Environ Sci Technol*, vol. 51, no. 12, 2017, doi: 10.1021/acs.est.7b00423.

[65] J. R. Rochester, "Bisphenol A and human health: A review of the literature," *Reproductive Toxicology*, vol. 42. 2013. doi: 10.1016/j.reprotox.2013.08.008.

[66] M. Cherif Lahimer, N. Ayed, J. Horriche, and S. Belgaied, "Characterization of plastic packaging additives: Food contact, stability and toxicity," *Arabian Journal of Chemistry*, vol. 10, 2017, doi: 10.1016/j.arabjc.2013.07.022.

[67] D. Brennecke, B. Duarte, F. Paiva, I. Caçador, and J. Canning-Clode, "Microplastics as vector for heavy metal contamination from the marine environment," *Estuar Coast Shelf Sci*, vol. 178, 2016, doi: 10.1016/j.ecss.2015.12.003.

[68] L. A. Holmes, A. Turner, and R. C. Thompson, "Interactions between trace metals and plastic production pellets under estuarine conditions," *Mar Chem*, vol. 167, 2014, doi: 10.1016/j.marchem.2014.06.001.

[69] L. A. Holmes, A. Turner, and R. C. Thompson, "Adsorption of trace metals to plastic resin pellets in the marine environment," *Environmental Pollution*, vol. 160, no. 1, 2012, doi: 10.1016/j.envpol.2011.08.052.

[70] F. Wang, J. Gao, W. Zhai, D. Liu, Z. Zhou, and P. Wang, "The influence of polyethylene microplastics on pesticide residue and degradation in the aquatic environment," *J Hazard Mater*, vol. 394, 2020, doi: 10.1016/j.jhazmat.2020.122517.

[71] A. Parthasarathy, A. C. Tyler, M. J. Hoffman, M. A. Savka, and A. O. Hudson, "Is Plastic Pollution in Aquatic and Terrestrial Environments a Driver for the Transmission of

Pathogens and the Evolution of Antibiotic Resistance?," *Environmental Science and Technology*. 2019. doi: 10.1021/acs.est.8b07287.

[72] "IMPTOX." https://www.imptox.eu/en/ (accessed Mar. 02, 2023).

[73] L. Eitzen, S. Paul, U. Braun, K. Altmann, M. Jekel, and A. S. Ruhl, "The challenge in preparing particle suspensions for aquatic microplastic research," *Environ Res*, 2019, doi: 10.1016/j.envres.2018.09.008.

[74] D. Choi, J. Bang, T. Kim, Y. Oh, Y. Hwang, and J. Hong, "In vitro chemical and physical toxicities of polystyrene microfragments in human-derived cells," *J Hazard Mater*, vol. 400, 2020, doi: 10.1016/j.jhazmat.2020.123308.

[75] X. Shi *et al.*, "Cytotoxicity and Genotoxicity of Polystyrene Micro-and Nanoplastics with Different Size and Surface Modification in A549 Cells," *Int J Nanomedicine*, vol. 17, 2022, doi: 10.2147/IJN.S381776.

[76] P. Li, Q. Li, Z. Hao, S. Yu, and J. Liu, "Analytical methods and environmental processes of nanoplastics," *Journal of Environmental Sciences (China)*, vol. 94. 2020. doi: 10.1016/j.jes.2020.03.057.

[77] H. Cai, E. G. Xu, F. Du, R. Li, J. Liu, and H. Shi, "Analysis of environmental nanoplastics: Progress and challenges," *Chemical Engineering Journal*, vol. 410, 2021, doi: 10.1016/j.cej.2020.128208.

[78] J. Seghers *et al.*, "Preparation of a reference material for microplastics in water—evaluation of homogeneity," *Anal Bioanal Chem*, vol. 414, no. 1, 2022, doi: 10.1007/s00216-021-03198-7.

[79] W. S. Lee, H. Kim, Y. Sim, T. Kang, and J. Jeong, "Fluorescent Polypropylene Nanoplastics for Studying Uptake, Biodistribution, and Excretion in Zebrafish Embryos," *ACS Omega*, vol. 7, no. 2, 2022, doi: 10.1021/acsomega.1c06779.

[80] C. Mayer-Laigle, N. Blanc, R. K. Rajaonarivony, and X. Rouau, "Comminution of dry lignocellulosic biomass, a review: Part I. from fundamental mechanisms to milling behaviour," *Bioengineering*, vol. 5, no. 2. 2018. doi: 10.3390/bioengineering5020041.

[81] G. Schubert and S. Bernotat, "Comminution of non-brittle materials," in *International Journal of Mineral Processing*, 2004. doi: 10.1016/j.minpro.2004.08.004.

[82] W. Müller, *Mechanische Verfahrenstechnik und ihre Gesetzmäßigkeiten*. 2014. doi: 10.1524/9783110343564.

[83] M. Wilczek, J. Bertling, and D. Hintemann, “Optimised technologies for cryogenic grinding,” in *International Journal of Mineral Processing*, 2004. doi: 10.1016/j.minpro.2004.07.032.

[84] V. Gente, F. La Marca, F. Lucci, P. Massacci, and E. Pani, “Cryo-comminution of plastic waste,” *Waste Management*, vol. 24, no. 7, 2004, doi: 10.1016/j.wasman.2004.03.005.

[85] S. Molina-Boisseau and N. Le Bolay, “Fine grinding of polymers in a vibrated bead mill,” in *Powder Technology*, 1999. doi: 10.1016/S0032-5910(99)00154-0.

[86] J. Schmidt, M. Plata, S. Tröger, and W. Peukert, “Production of polymer particles below 5µm by wet grinding,” *Powder Technol*, vol. 228, 2012, doi: 10.1016/j.powtec.2012.04.064.

[87] L. Z. Zuo *et al.*, “Sorption and desorption of phenanthrene on biodegradable poly(butylene adipate co-terephtalate) microplastics,” *Chemosphere*, vol. 215, 2019, doi: 10.1016/j.chemosphere.2018.09.173.

[88] S. Kühn, A. van Oyen, A. M. Booth, A. Meijboom, and J. A. van Franeker, “Marine microplastic: Preparation of relevant test materials for laboratory assessment of ecosystem impacts,” *Chemosphere*, vol. 213, 2018, doi: 10.1016/j.chemosphere.2018.09.032.

[89] F. Corradini, H. Bartholomeus, E. Huerta Lwanga, H. Gertsen, and V. Geissen, “Predicting soil microplastic concentration using vis-NIR spectroscopy,” *Science of the Total Environment*, vol. 650, 2019, doi: 10.1016/j.scitotenv.2018.09.101.

[90] X. Guo, J. Pang, S. Chen, and H. Jia, “Sorption properties of tylosin on four different microplastics,” *Chemosphere*, vol. 209, 2018, doi: 10.1016/j.chemosphere.2018.06.100.

[91] H. El Hadri, J. Gigault, B. Maxit, B. Grassl, and S. Reynaud, “Nanoplastic from mechanically degraded primary and secondary microplastics for environmental assessments,” *NanoImpact*, vol. 17, 2020, doi: 10.1016/j.impact.2019.100206.

[92] K. Ravishankar, P. S. Ramesh, B. Sadhasivam, and D. Raghavachari, “Wear-induced mechanical degradation of plastics by low-energy wet-grinding,” *Polym Degrad Stab*, vol. 158, 2018, doi: 10.1016/j.polymdegradstab.2018.10.026.

[93] J. T. Jung, J. F. Kim, H. H. Wang, E. di Nicolo, E. Drioli, and Y. M. Lee, “Understanding the non-solvent induced phase separation (NIPS) effect during the fabrication of

microporous PVDF membranes via thermally induced phase separation (TIPS)," *J Memb Sci*, vol. 514, 2016, doi: 10.1016/j.memsci.2016.04.069.

[94] "Hemocytometer.org." https://www.hemocytometer.org/hemocytometer-calculation/#manually (accessed Jun. 10, 2023).

I have made every effort to locate all owners of the image rights and have obtained their permission to use the images in this work. Should a copyright infringement nevertheless become known, I request that you notify me.

Appendix

Zusammenfassung

Bereits seit einiger Zeit wurde die globale Plastikverschmutzung als globales Problem anerkannt. Zuletzt hat sich der Fokus jedoch auf die Verschmutzung durch Mikro- und Nanoplastik (MNP) verschoben. Diese kleinen Partikel werden entweder gezielt hergestellt oder sind (häufiger) das Ergebnis eines Zerkleinerungsprozesses durch verschiedene Umwelteinflüsse. Diese Partikel sind mittlerweile in jedem Teil der Erde zu finden und stellen möglicherweise ein großes Risiko für die menschliche Gesundheit dar. Das Wissen über die genauen Auswirkungen, ist jedoch aufgrund eines Mangels an standardisierten Testmaterialien sehr begrenzt. Dies gilt insbesondere für die am häufigsten im Menschen gefundenen Polymertypen wie Polypropylen (PP).

Im Rahmen dieser Masterarbeit wurden zwei Ansätze zur Herstellung von PP-Partikeln in drei verschiedenen Größenklassen untersucht. Der Hauptteil der Arbeit lag in der Optimierung und Untersuchung der Reproduzierbarkeit eines Nassmahlverfahrens zu Herstellung von PP-Partikeln im Bereich von 1-10 µm (M-Fraktion) und 10-38 µm (L-Fraktion). Dieser Prozess bestand aus einem anfänglichen Mahlverfahren, gefolgt von drei verschiedenen Schritten zur Größenunterteilung. Dazu gehörten das Sieben des Materials, das Filtrieren und ein Zentrifugationsschritt. Abschließend wurde ein Austausch des Suspensionsmediums vollzogen. Die Reproduzierbarkeit des Verfahrens wurde getestet, indem der ganze Prozess insgesamt fünfmal durchgeführt wurde. Darüber hinaus kam eine Methode namens „non-solvent induced phase separation“ (NIPS) für die Produktion von Nanopartikeln in der Größenordnung 0,1 – 1 µm zum Einsatz. Die Partikelgrößenverteilungen und Perzentile dieser Verteilungen wurden mithilfe von Laser-Diffraktion gemessen. Die Ausbeute der Produkte wurde mittels gravimetrischer Messung und durch händische Partikelauszählung mittels eines Lichtmikroskops bestimmt.

Die Optimierung des Mahlprozesses zeigte, dass Partikel in den gewünschten Größenklassen (L- und M-Fraktion) hergestellt werden können. Die anschließende Prüfung auf Reproduzierbarkeit ergab ein hohes Maß an Reproduzierbarkeit für die L-Fraktion (Mittlere Perzentile der finalen L-Fraktion: D90: 58,78 µm ± 6,33 %; D50: 27,76 µm ± 4,91 %; D10: 9,35 µm ± 4,22 %). Im Gegensatz dazu, wies der Prozess zur Herstellung der M-Fraktion eine unzureichende Reproduzierbarkeit auf (Mittlere

Perzentile der finalen M-Fraktion: D90: 45,36 µm ± 19,12 %; D50: 12,29 µm ± 10,74 %; D10: 4,01 µm ± 9,81 %). Die finale Ausbeute beider Fraktionen war äußerst gering und zeigte keine ausreichende Reproduzierbarkeit (L-Fraktion: 3,32 mg ± 26,99 %; M-Fraktion: 0,91 mg ± 33,59 %). Die NIPS-Methode zeigte, dass die Herstellung von PP-NPs, in ausreichenden Mengen möglich ist (Mittlere Perzentile: D90: 43,42 µm ± 52,66%; D50: 2,62 µm ± 63,45%; D10: 0,312 µm ± 15,49%). Im Gegensatz zum Mahlverfahren waren bei dieser Methode die Ausbeuten einheitlicher und die relative Ausbeute von 89,85% ± 2,42 % (245,74 mg) wesentlich höher. Diese Arbeit zeigt, dass es möglich ist, PP-MNPs in den gewünschten Größenordnungen mit einem gewissen Grad an Reproduzierbarkeit herzustellen.